Evaluation of the Buchanan County IBRD Bridge on Victor Avenue over Prairie Creek

Final Report
September 2017

BRIDGE ENGINEERING CENTER

IOWA STATE UNIVERSITY

Institute for Transportation

About the Bridge Engineering Center

The mission of the Bridge Engineering Center (BEC) is to conduct research on bridge technologies to help bridge designers/owners design, build, and maintain long-lasting bridges.

About the Institute for Transportation

The mission of the Institute for Transportation (InTrans) at Iowa State University is to develop and implement innovative methods, materials, and technologies for improving transportation efficiency, safety, reliability, and sustainability while improving the learning environment of students, faculty, and staff in transportation-related fields.

Disclaimer Notice

Iowa State University Non-Discrimination Statement

Iowa Department of Transportation Statements

Technical Report Documentation Page

1. Report No. InTrans Project 12-427	2. Government Accession No.	3. Recipient's Catalog No.	
4. Title and Subtitle Evaluation of the Buchanan County IBRD Bridge on Victor Avenue over Prairie Creek		**5. Report Date** September 2017	
		6. Performing Organization Code	
7. Author(s) Brent Phares (orcid.org/0000-0001-5894-4774), Travis Hosteng (orcid.org/0000-0002-2059-1296), Lowell Greimann (orcid.org/0000-0003-2488-6865), and Anmol Pakhale (orcid.org/0000-0002-8888-2276)		**8. Performing Organization Report No.** InTrans Project 12-427	
9. Performing Organization Name and Address Bridge Engineering Center Iowa State University 2711 South Loop Drive, Suite 4700 Ames, IA 50010-8664		**10. Work Unit No. (TRAIS)**	
		11. Contract or Grant No.	
12. Sponsoring Organization Name and Address Iowa Department of Transportation 800 Lincoln Way Ames, IA 50010	FHWA Innovative Bridge Research and Deployment (IBRD) Program 1200 New Jersey Avenue, SE Washington, DC 20590	**13. Type of Report and Period Covered** Final Report	
		14. Sponsoring Agency Code IBRD	

15. Supplementary Notes

Visit www.intrans.iastate.edu for color pdfs of this and other research reports.

16. Abstract

With the assistance of the Iowa Department of Transportation (DOT) and three centers at the Institute for Transportation (InTrans) at Iowa State University, Buchanan County, Iowa was awarded a Federal Highway Administration (FHWA) Innovative Bridge Research and Deployment (IBRD) Program grant to help construct and evaluate a replacement bridge that used innovative concepts to increase the bridge's durability, while also striving to construct the bridge without the use of a traditional overhead crane, making the bridge system an attractive alternative for county workforces and minimizing disruption to the traveling public.

The innovative concepts utilized for this bridge included geosynthetic-reinforced soil (GRS) abutments, high-performance concrete (HPC) with lightweight fine aggregates (LWFAs) for internal curing, and a cast-on-site concrete box-beam superstructure.

Conclusions from the project included the following:

- The use of LWFAs to internally cure the concrete leads to higher strength of concrete and slightly lower weight of the beams.

- Lifting the beams from both ends using two backhoes and moving the beams over the creek was a successful approach and did not cause any damage to the beams beyond some minor bottom flange cracking.

- The load tests performed on the bridge over three years indicated that the bridge joints are well connected and performing well.

- The construction of the beams on-site followed by moving them over the abutments was a time-saving approach, which led to less traffic disruption.

- The GRS abutments did not show any erosion of backfill or any other issues after a flood event occurred in the spring of 2015.

- Results showed that the installation of the vertical sheet drain in one of the abutments provided improved drainage conditions over the abutment without the vertical sheet drain.

17. Key Words bridge reconstruction—cast-on-site bridges—geosynthetic-reinforced soil abutments—high-performance concrete—innovative bridge replacement—internal concrete curing—vertical sheet drains		18. Distribution Statement No restrictions.	
19. Security Classification (of this report) Unclassified.	**20. Security Classification (of this page)** Unclassified.	**21. No. of Pages** 71	**22. Price** NA

Form DOT F 1700.7 (8-72)   **Reproduction of completed page authorized**

Evaluation of the Buchanan County IBRD Bridge on Victor Avenue over Prairie Creek

Final Report
September 2017

Principal Investigator
Brent Phares, Director
Bridge Engineering Center

Co-Principal Investigators
Peter Taylor, Director
National Concrete Pavement Technology Center

Pavana Vennapusa, previous Research Assistant Professor
Center for Earthworks Engineering Research, Iowa State University

Research Assistant
Anmol Pakhale

Authors
Brent Phares, Travis Hosteng, Lowell Greimann, and Anmol Pakhale

A report from
**Bridge Engineering Center and
Institute for Transportation
Iowa State University**
2711 South Loop Drive, Suite 4700
Ames, IA 50010-8664
Phone: 515-294-8103 / Fax: 515-294-0467
www.intrans.iastate.edu

TABLE OF CONTENTS

LIST OF FIGURES

LIST OF TABLES

ACKNOWLEDGMENTS

EXECUTIVE SUMMARY

Recently, there has been increased interest in constructing bridges that last longer, are less expensive, and take less time to construct. The idea is to generally increase the cost-effectiveness of bridges by increasing their durability (i.e., useful life) and minimizing construction disruptions to the traveling public.

With the assistance of the Iowa Department of Transportation (DOT) and three centers at the Institute for Transportation (InTrans) at Iowa State University, Buchanan County, Iowa was awarded a Federal Highway Administration (FHWA) Innovative Bridge Research and Deployment (IBRD) Program grant to help construct and evaluate a replacement bridge that used innovative concepts, while also striving to construct the bridge without the use of a traditional overhead crane, making the bridge system an attractive alternative for county workforces.

The innovative concepts utilized for this bridge included geosynthetic-reinforced soil (GRS) abutments, high-performance concrete (HPC) made with lightweight fine aggregate (LWFA) for internal curing, and a cast-on-site concrete box-beam superstructure.

This project consisted of four major tasks to encompass its objectives.

- Preliminary design support and documentation

  To support Buchanan County and the Iowa DOT Office of Bridges and Structures, the Iowa State University team assisted with the preliminary bridge design process. Specifically, the research team assisted Buchanan County with the design of the GRS abutments and the Office of Bridges and Structures with the superstructure design.

  The project involved the replacement of an aged timber bridge (the Slattery Bridge) with a cast-on-site adjacent box beam bridge. The replacement bridge is 50 ft long and 30 ft wide with a 0-degree skew. The bridge is located on Victor Avenue over Prairie Creek in Buchanan County.

  The replacement bridge was designed for HL-93 loading plus 20 lb/ft^2 for a future wearing surface. It consists of precast box beams and guardrails with a GRS abutment and a sheet pile foundation system. Each of the five precast concrete beams is 6 ft wide, creating the 30 ft bridge width.

- Testing of concrete materials and mix used for the beams

  HPC (with LWFAs for internal curing) was used to fabricate the precast beams on site. The research team performed laboratory tests on the concrete mix that was used and coordinated the results with both Buchanan County and the Iowa DOT.

- Construction inspection and documentation

  The research team assisted the Office of Bridges and Structures with inspection of key phases of bridge construction. The construction process was observed and documented using digital images. Of particular interest was the fabrication of the precast bridge components, GRS abutment construction, and placement of the prefabricated superstructure on the GRS abutments.

- Bridge inspection

  After the construction of the bridge, its performance was monitored for three consecutive years (2014, 2015, and 2016) via live load tests and other data collection mechanisms. The research team mounted external instrumentation for each load test and carried out the tests. The data from pore pressure sensors in the GRS abutments were also collected with all data analyzed to evaluate the structural performance of the bridge.

Key Findings

- The use of LWFAs for the concrete leads to higher strength of concrete and slightly lower weight of the beams.

- The beam weight was too heavy for the tow truck to slide or lift and led to some minor damage of the test girder.

- Lifting the beams from both ends using two backhoes and moving the beams over the creek was a successful approach and did not cause any damage to the beams beyond some minor bottom flange cracking.

- The load tests performed on the bridge over three years indicated that the bridge joints are well connected and performing well.

- The GRS abutments did not show any erosion of backfill or any other issues after a flood event occurred in the spring of 2015.

Implementation Readiness and Benefits

- Using backhoes to lift the cast-on-site beams is recommended.

- The lifting of the cast-on-site beams using backhoes may have a limit of span length, which should be investigated.

- The construction of the beams on-site followed by moving them over the abutments was a time-saving approach, which led to less traffic disruption.

- Concrete should be cured internally in addition to the external curing.

- Results showed that the installation of the vertical sheet drain in one of the abutments provided improved drainage conditions over the abutment without the vertical sheet drain.

- Long-term visual monitoring of these two abutments is recommended to see how they perform with additional flood events. A proper scour design was not performed for this site, although the sheet piles were extended at least 5 ft into the very stiff foundation layer. Scouring near the bottom of the sheet piles should be monitored over time.

Future Research

- The method of cast-on-site beams should be attempted and tested for a longer span or multiple-span bridge.

- A bridge constructed using the philosophy of "get in, get out, stay out" should be inspected for structural soundness for a longer time period.

- The GRS benefits with the inclusion of vertical sheet drains should be further studied for a broader impact using different backfill materials that are typically used in Iowa, with varying fines content and particle size distributions.

1   Introduction

1.1   Background

"Nearly half—more than 250,000—of US bridges, according to the National Bridge Inventory, are in the 25 to 50 year age range. This is a major concern for many state departments of transportation (DOTs) and the Federal Highway Administration (FHWA) because many bridges have a life expectancy of 50 years—making them near the ends of their anticipated life cycles. The current goal with new bridge construction is a 100-year lifespan.

In addition to aging, about 26 percent of the bridges in the US are deficient. Highway capacity also has increased little during the past two decades, but traffic demand has grown tremendously, causing increased congestion, with bridge construction projects compounding the problem. Traffic control represents anywhere from 20 to 40 percent of construction costs, and user delays are priced at thousands of dollars per day in heavy traffic areas." Mistry and Mangus 2006.

There has been increased interest in constructing bridges with longer life spans, less construction time, and lower costs for traffic control and user delays. This approach is basically known as the get in, get out, stay out philosophy. The first two portions of the philosophy are self explanatory. The "stay out" portion refers to the inherent lasting quality of prefabricated components that are produced in the controlled environment of a fabrication site.

To accomplish this philosophy in this project, several innovative concepts were included. A bridge in Buchanan County, Iowa that needed replacement was chosen for this project. The bridge was constructed in Buchanan County with the assistance of the Iowa Department of Transportation (DOT) and the Iowa State University Bridge Engineering Center (BEC), National Concrete Pavement Technology (CP Tech) Center, and Center for Earthworks Engineering Research (CEER).

The bridge was constructed with three innovative concepts. The bridge foundation consisted of geosynthetic-reinforced soil (GRS) abutments and concrete caps. The GRS abutments were designed by Buchanan County with assistance by the research team. One abutment was provided with geocomposite drainage system while other one was without the geocomposite drainage system. After the construction of the GRS abutments, their performance was monitored with pore pressure sensors installed on both abutments.

The superstructure of the bridge consisted of five prefabricated beams. These beams were fabricated on site by the creek over which the bridge was to be constructed. The beams were constructed with high performance concrete (HPC) with internal curing. Internal curing prolongs the cement hydration by providing internal water reservoirs through the lightweight aggregate and also in turns decreases the weight/density of the beam by use of lightweight aggregates.

Strain gages were mounted on the reinforcement of the prefabricated beams to record the strain when moving them. The beams were moved over the creek using two cranes. The strains in the

beam were recorded in different locations to determine the impacts of the move on the beams' structural soundness. After the beams were placed over the concrete abutments, the bridge was then monitored for three years for its structural performance with live load tests.

1.2 Objectives

This project consisted of four major tasks to encompass its objectives.

- Preliminary design support and documentation

  To support Buchanan County and the Iowa DOT Office of Bridges and Structures, the Iowa State University team assisted with the preliminary bridge design process. Specifically, the research team assisted Buchanan County with the design of the GRS abutments and the Office of Bridges and Structures with the superstructure design.

- Testing of concrete materials and mix used for the beams

  HPC (made with lightweight fine aggregates [LWFAs] for internal curing) was used to fabricate the precast beams on site. The research team performed laboratory tests on the concrete mix that was used and coordinated the results with both Buchanan County and the Iowa DOT.

- Construction inspection and documentation

  The research team assisted the Office of Bridges and Structures with inspection of key phases of bridge construction. The construction process was observed and documented using digital images. Of particular interest was the fabrication of the precast bridge components, GRS abutment construction, and placement of the prefabricated superstructure on the GRS abutments.

- Bridge inspection

  After the construction of the bridge, its performance was monitored for three consecutive years (2014, 2015, and 2016) via live load tests and other data collection mechanisms. The research team mounted external instrumentation for each load test and carried out the tests. The data from pore pressure sensors in the GRS abutments were also collected with all data analyzed to evaluate the structural performance of the bridge.

1.3 Report Content

This report consists of four chapters subdivided into various sections. The first chapter of the report is an introduction to the project including the objectives. The second chapter consists of the bridge description including the design of the bridge, a description of the internal curing concrete used in the superstructure, and documentation of the construction of the bridge. The third chapter assesses the evaluation of the bridge through the data collected. The fourth chapter includes the conclusions drawn from the study and recommendations developed as a result.

2   BRIDGE DESCRIPTION

2.1   General Information

The project involved the replacement of an aged timber bridge (the Slattery Bridge) with a cast-on-site adjacent box beam bridge. The replacement bridge is 50 ft long and 30 ft wide with a 0-degree skew. The bridge is located on Victor Avenue over Prairie Creek in Buchanan County, Iowa, as shown in Figure 1.
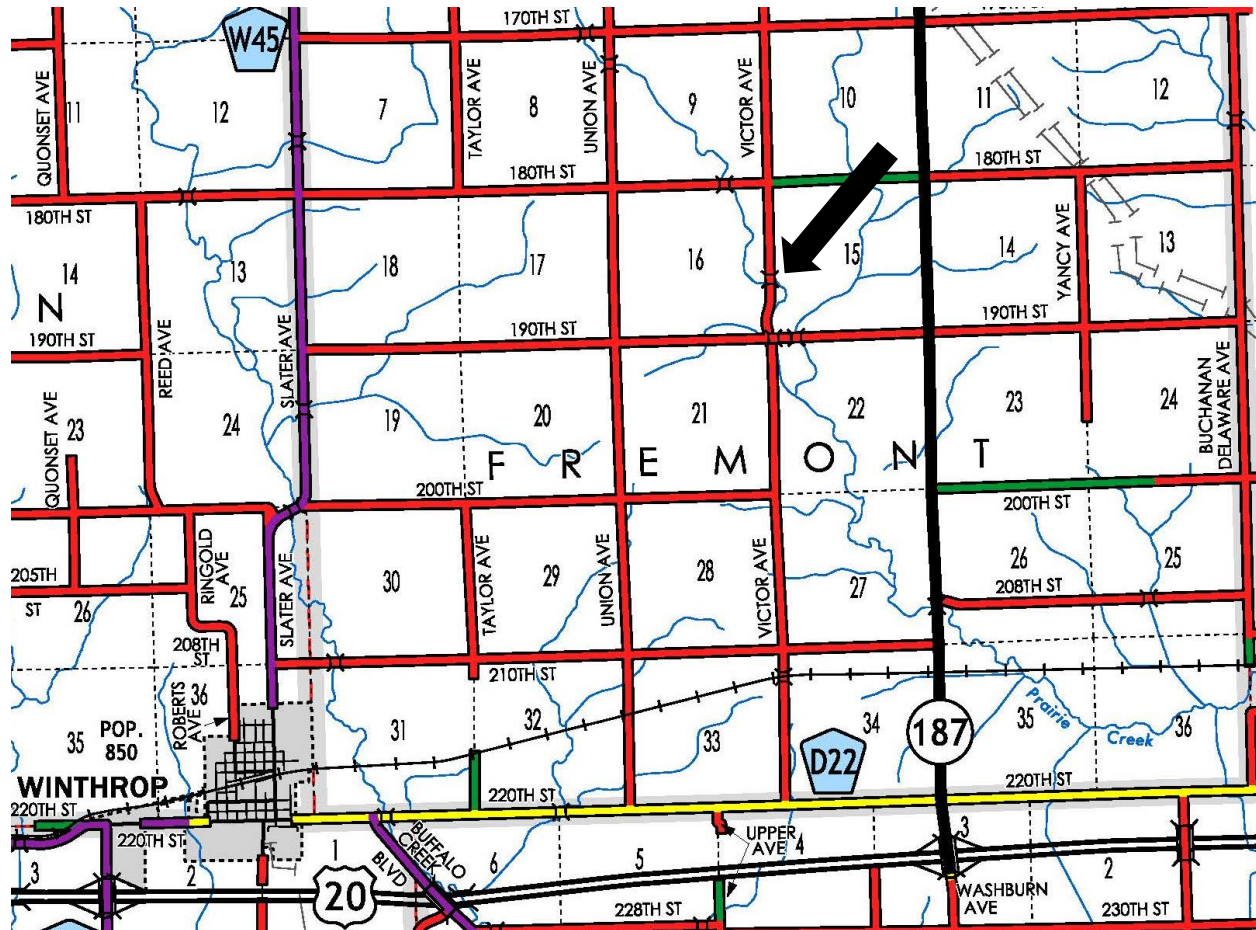
Iowa DOT Buchanan County Highway and Transportation Map (T-89-N, R-7W on map and in Section 15 of Fremont Township)

Figure 1. Location of Victor Avenue bridge over Prairie Creek in Buchanan County, Iowa

The replacement bridge was designed for HL-93 loading plus 20 lb/ft^2 for a future wearing surface. It consists of precast box beams and guardrails with a GRS abutment and a sheet pile foundation system. Each of the five precast concrete beams is 6 ft wide, creating the 30 ft bridge width. Figure 2 shows a plan and elevation view of the bridge.

a. Plan
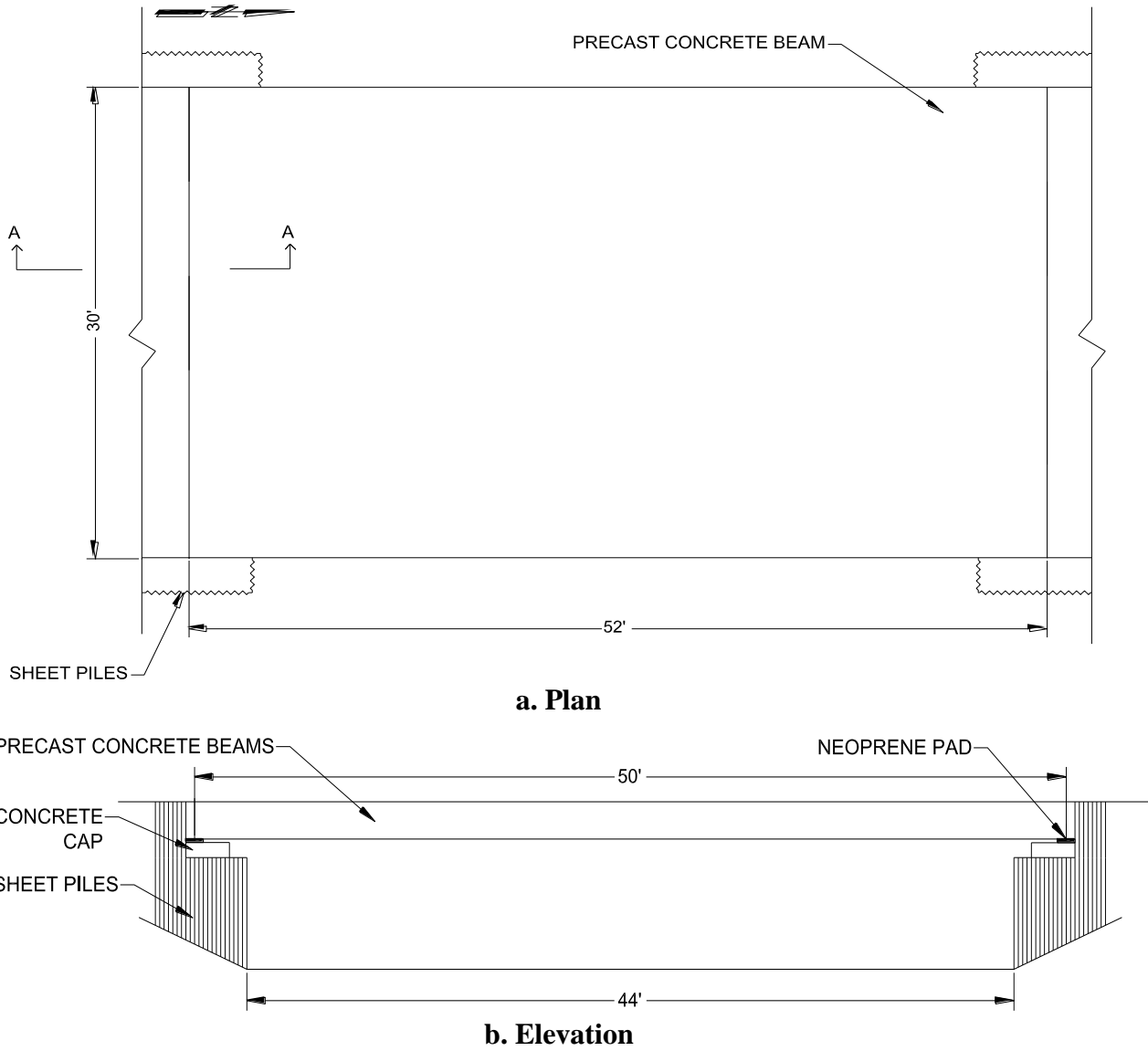
b. Elevation

Figure 2. Plan and elevation views of the bridge

Figure 3 shows a cross-sectional view of the substructure including details of the GRS abutments and concrete caps.
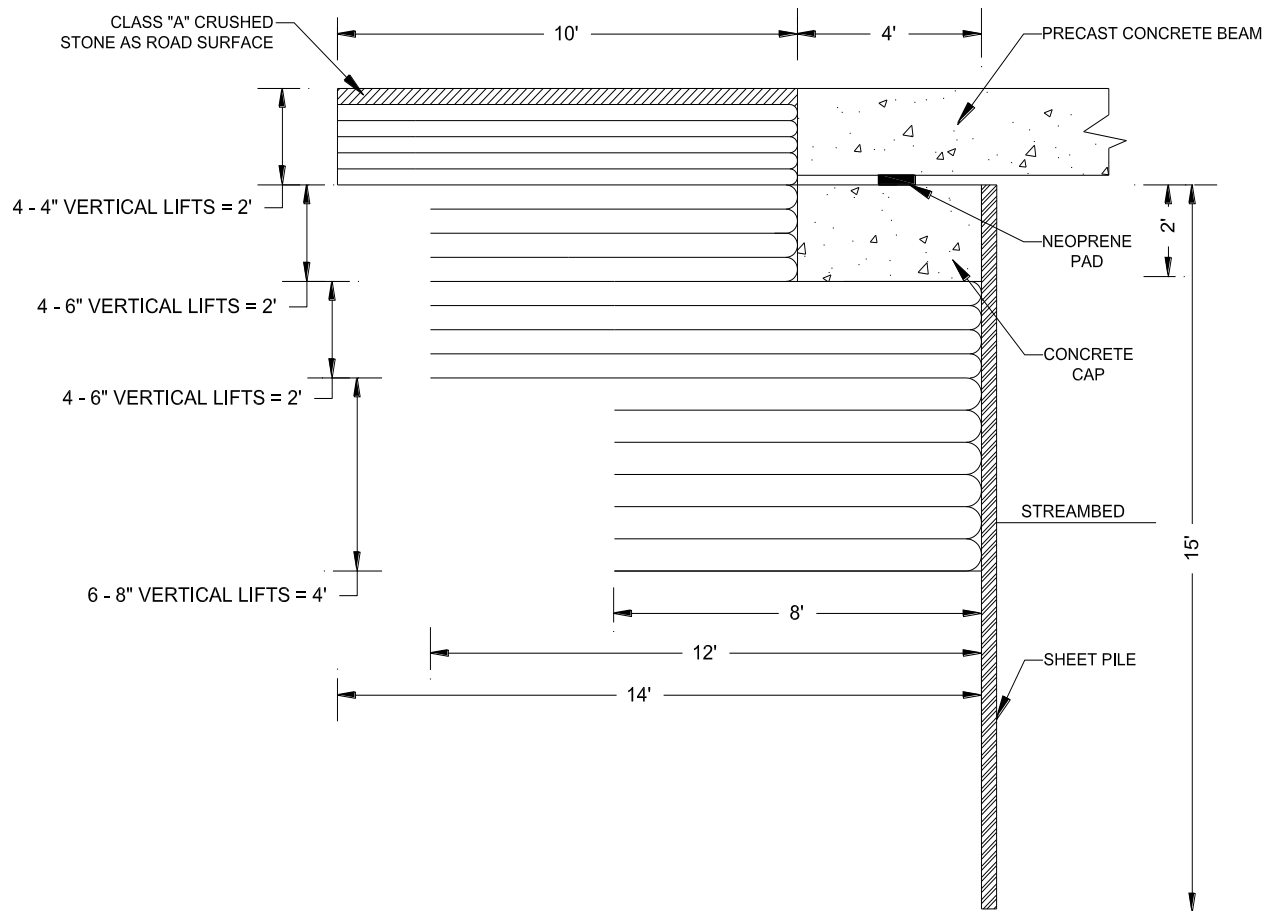
Figure 3. Abutment details (Section A-A)

As shown, four different configurations of granular material and fabric with different lengths make up the GRS abutments. The vertical lifts of granular material start just below the streambed and continue vertically to the bottom of the crushed stone road surface. The ends of the vertical lifts towards the streambed are protected by steel sheet piles, designed to improve external stability of the abutment backfill and also serve as facing elements to help avoid erosion of backfill materials and scouring. The sheet piles are driven to 8 ft below the streambed to provide stability.

A concrete cap is placed on top of the granular material and fabric, as shown in Figure 3, which then supports the precast concrete beams and transfers load to the substructure. This reinforced concrete cap is 4 ft wide, 2 ft high and 34 ft in length. A 1 in. by 8 in. neoprene pad is placed between the concrete cap and the concrete beams. The neoprene is placed with its centerline about one foot from each end of each beam.

The vertical lifts behind the concrete beams extend 10 ft past the concrete beam to provide support to the road leading to the bridge. The road surface consists of Class A crushed stone.The bridge superstructure consists of five precast concrete box beams that are 2 ft high by 6 ft wide

5

by 52 ft long (Figure 4 and Figure 5). Figure 4 shows the as-designed plan view of one beam for one-half of each beam. In this figure, the longitudinal reinforcement is not shown to improve clarity.
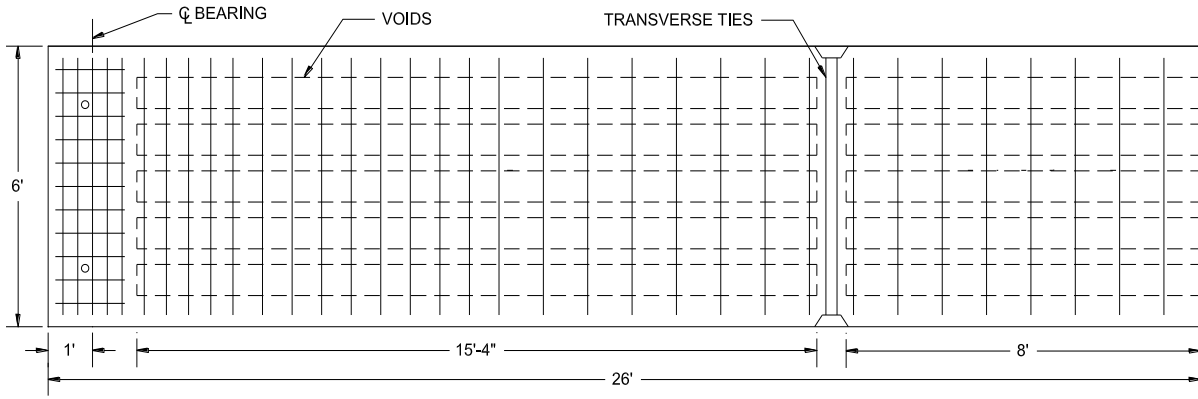
Figure 4. Sectional plan view of beam

Figure 5 shows an as-designed elevation view of the beam.
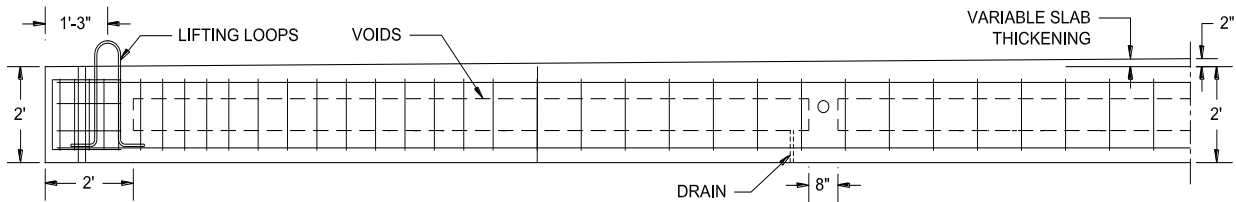
Figure 5. Sectional elevation view of beam

There were two lifting loop provided on each end of the beam. To accommodate the dead load deflection at midspan, a variable thickness top flange was provided.

To connect adjacent boxes, grouted shear keys were provided at the longitudinal joints between adjacent girders to ensure a load-sharing mechanism. Per the design plans, keyway grout with 5.0 ksi compressive strength at 24 hours was to be used to fill the shear key. Figure 6 shows the bridge cross-section at a typical transverse tie.
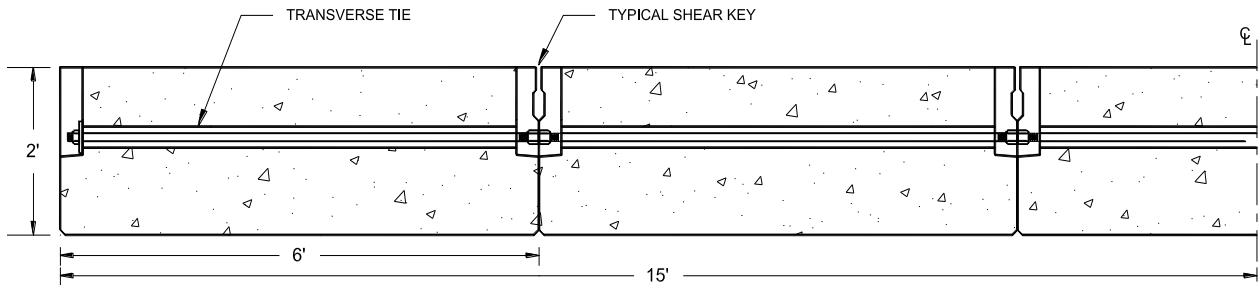
Figure 6. Deck cross-section at the transverse ties

Figure 7a shows the as-designed beam cross-section at the centerline of bearing while Figure 7b shows the beam cross-section at midspan. In this figure five 8 in. diameter voids placed 5 in. (end to end) apart are shown. Every void was to be provided with a drain for water as shown in Figure 7b. It should be noted that the contractor elected to not include the voids in the box beams.
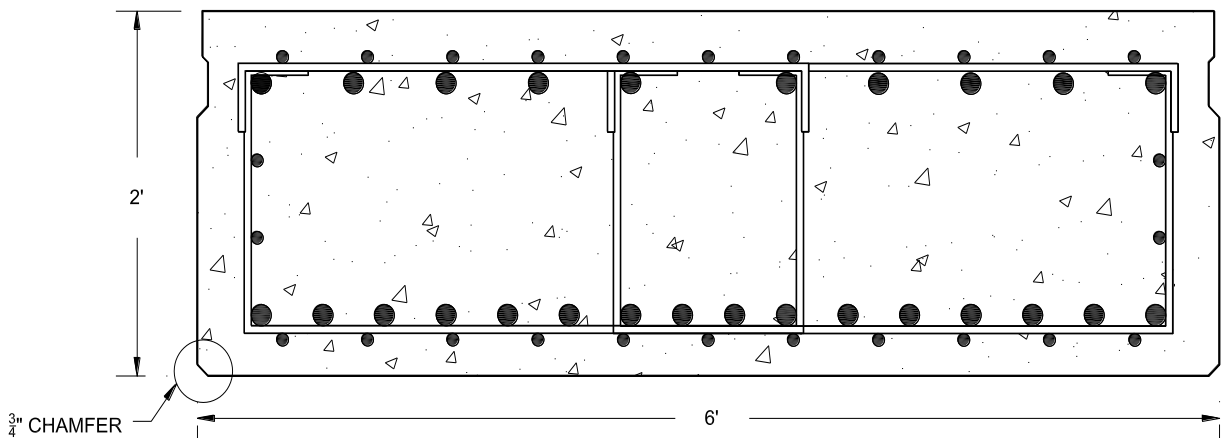
a. Beam cross-section at centerline of bearing
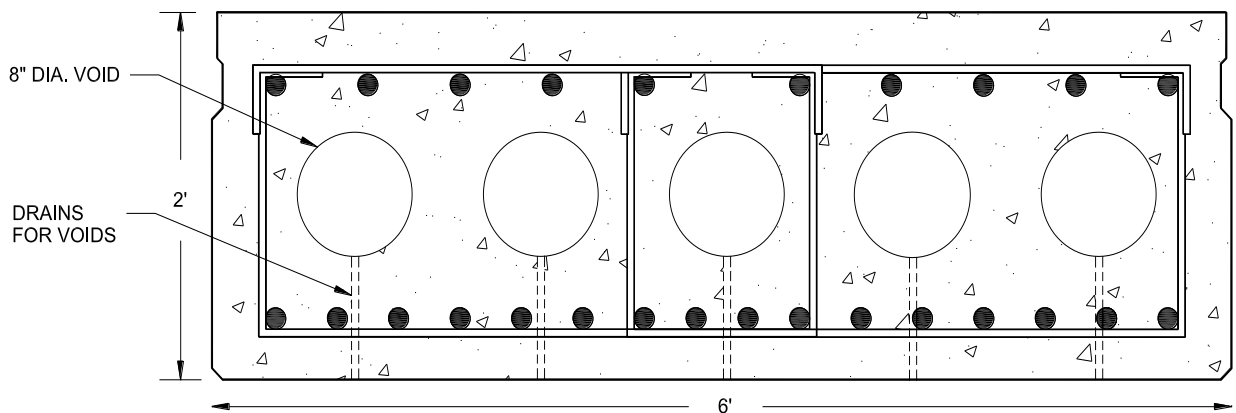
b. Beam cross-section at midspan

Figure 7. Beam interior span sections

2.2 GRS Abutment Design

GRS is an engineered fill with closely-spaced alternating layers of compacted granular fill material and geosynthetic reinforcement. Due to the friction developed at the granular soil-geosynthetic interface, the reinforcement restrains lateral deformation of the surrounding soil, increases its confinement, reduces its tendency to dilation, and also increases the strength and stiffness of the soil (Adams et al. 2011a).

According to FHWA GRS design guidelines (Adams et al. 2011b), the bearing stress on the GRS fill should be limited to 4,000 lb/ft^2 and the reinforcement layer spacing should be limited to 12 in. or less. GRS design starts with establishing the project requirements from which the preliminary geometry is determined and then evaluated against external and internal modes of failure. An iterative process is used to assess the geometry and make adjustments as necessary to facilitate construction and assure long-term performance.

The external stability in the GRS-integrated bridge system (GRS-IBS) design method is similar to checking the external stability of any other abutment systems, i.e., checking for stability against direct sliding at the interface of GRS fill material and foundation soil, bearing capacity of the foundation soils supporting GRS fill material, and global stability (either wedge or rotational) against failure (Berg et al. 2009). The FHWA design guidelines for GRS recommend the minimum factor of safety against sliding (FSsliding) is 1.5, bearing capacity (FSbearing) is 2.5, and global stability (FSstability) is 1.5.

Soil borings were performed by Buchanan County at this site (one on each abutment side) and the profiles are included in the appendix. Both borings were performed on the south side of existing abutments in the native material. The profiles showed dark brown silty to clayey sand up to a depth of about 7 ft, underlain by about 7 to 10 ft of a stiff sandy lean clay layer, and a very stiff sandy lean clay layer down to the boring termination depths of about 51 to 52 ft.

Laboratory soil classification test results, moisture and dry density, and unconfined compressive (UC) strength test results obtained from the Shelby tube and split spoon samples provided Buchanan County are presented in the boring logs. The results were used in analyzing the external stability of the designed structure, which showed factor of safety values that exceed the minimum values recommended as stated above.

A summary of the global slope stability analysis performed for various water table elevation cases and different sheet pile lengths is provided in the appendix. Results showed that the rapid drawn down case presents the worst case scenario and extending the sheet pile down at least 5 ft into the very stiff sandy clean layer was needed. The design sheet pile length depicted previously in Figure 3 represents this case.

The internal stability analysis of GRS abutment systems involve evaluating ultimate bearing capacity and required reinforcement strength. The analytical approach to estimate ultimate bearing capacity per Adams et al. (2011b) involves using equation (1):

$$q_{ult} = \left[0.7^{\left(\frac{s_v}{6d_{max}} \right)} \frac{T_f}{s_v} \right] K_{pr}$$

(1)

where, s_v = reinforcement spacing vertically, d_{max} = maximum particle size of the granular backfill material, T_f = ultimate strength of the reinforcement (determined from ASTM D4595 and is typically reported by the manufacturer), and K_{pr} = coefficient of passive earth pressure determined using equation (2):

$$K_{pr} = \tan^2 \left(45 + \frac{\varphi'_r}{2} \right)$$

(2)

where ϕ'_r = angle of shearing resistance of the reinforced fill material. Adams et al. (2011a) report that ultimate bearing capacities estimated using the analytical approach compared well with results obtained from full-scale experiments and in-service GRS structures. The recommended factor of safety against internal bearing capacity (FSGRSbearing) = 3.5.

The geosynthetic material used in this study was Mirafi HP570 woven with a T_f = 4,800 lbs/ft. Based on prior laboratory testing results documented by Vennapusa et al. (2012) on similar granular material (classified as GW with crushed limestone with 1 in. maximum particle size), the ϕ'_r is conservatively assumed as 35°. Based on these values, the FSGRSbearing was greater than 3.5 for the loading conditions at this site.

The required reinforcement strength (T_{req}) can be determined using equation (3):

$$T_{req} = \left[\frac{\sigma_h}{0.7^{\left(\frac{s_v}{6d_{max}} \right)}} \right] s_v$$

(3)

where, σ_h = total lateral stress within the GRS fill material at a given depth and location, which includes contribution from all dead and live loads over the GRS fill material:

The T_{req} must satisfy two criteria: (1) it must be less than the allowable reinforcement strength (T_{all}) and (2) it must be less than strength at 2% reinforcement strain. T_{all} is calculated as the ratio of reinforcement ultimate strength, T_f, divided by factor of safety = 3.5. The reinforcement lengths shown previously in Figure 3 satisfy this requirement.

During construction, one change from the actual design was implemented on the south abutment. This change included addition of a sheet drain between the GRS fill and the sheet pile. The objective of this inclusion was to assess if the sheet drain on the south abutment provides any

extra drainage during a flood event than the abutment without the sheet drain (north abutment). Additional details about this are presented in Section 2.4.

2.3   Internal Curing Concrete

Curing plays a vital role in achieving high quality concrete elements. Cement hydration is a series of complex chemical reactions that require an adequate water supply and proper temperatures over an extended time (Taylor 2014). Curing is defined as "action taken to maintain moisture and temperature conditions in a freshly placed cementitious mixture to allow hydraulic cement hydration and (if applicable) pozzolanic reactions to occur so that the potential properties of the mixture may develop" (ACI 2016).

Conventional concrete is typically cured using so-called external methods. External curing prevents drying of the surface, allows the mixture to stay warm and moist, and results in continued cement hydration (Taylor 2014). Internal curing is a relatively new curing technique that has been developed to prolong the cement hydration process by providing internal water reservoirs in a concrete mixture that do not adversely affect the concrete mixture's fresh or hardened physical properties. Internal curing grew out of the need for more durable structural concretes that were resistant to shrinkage cracking (Babcock and Taylor 2015).

High performance concrete (made with LWFAs for internal curing) was used to fabricate the precast Victor Avenue bridge beams. Table 1 shows the details of the mix design.

Table 1. Mix design for high performance concrete with internal curing

Material	Moisture Content (%)	Bulk Density (lb/ft^3)	Loose Volume (ft^3)	Dry Weight (lbs)	Batch Weight (lbs)	Specific Gravity	Absolute Volume (ft^3)
Portland Cement	--	94.0	3.79	356	356	3.15	1.81
GGBFS	--	80.0	1.48	119	119	2.93	0.65
Fly Ash (Class C)	--	75.0	1.58	119	119	2.68	0.71
Coarse Aggregate	1.5%	95.0	15.60	1,482	1,504	2.62	9.06
Sand Fine Aggregate	3.0%	107.0	9.73	1,041	1,072	2.65	6.29
Buildex Fine Aggregate	21.0%	6'1.9	4.80	302	311	1.75	2.77
Water	--	62.4	3.56	--	222	1.00	3.56
Aggregates Surface Moisture	--	62.4	0.53	--	33	1.00	0.53
Air Content @6.0%	--	--	--	--	--	--	1.62
MRWR Admixture	--	--	--	--	--	--	--
Total Materials					3,702		27.00

The 28-day average compressive strength of the concrete was 6,870 psi (ASTM C39), which was higher than the required strength of 4,000 psi and the surface resistivity was 13.90 kΩ-cm, which is considered in the moderate range (AASHTO TP 95). Due to the use of the lightweight aggregate for internal curing processes, the beam weighed about 5% lighter than had the beam been fabricated using conventional concrete.

Table 2 and Table 3 show the fresh properties required for the mix.

Table 2. Fresh properties for high performance concrete with internal curing (air content and slump)

Property	As mixed	At placement
Air content	6.00%	4.5% to 5%
Slump	5" to 6"	4" to 5"

Table 3. Fresh properties for high performance concrete with internal curing (density and w/c ratio)

Property	Value
Fresh concrete density (before pumping)	137.1 lbs/ft^3
Fresh concrete density (after pumping)	138.6 lbs/ft^3
Water/cementitious materials ratio	0.43

2.4   Construction

2.4.1   GRS Abutments

The construction of the GRS abutments involved first installing the sheet piles to the design length and excavating the material to about 10 ft below the final bridge elevation. The excavation elevations were monitored using a robotic total station during construction. Excavation of the north abutment is shown in Figure 8.

Figure 8. Excavation of the GRS backfill area after installing sheet pile abutments

A 6 in. perforated drain tile was installed around the sheet pile, near the bottom of the excavation on a bed of porous backfill material (see Figure 9).

Figure 9. Placement of porous backfill material around the sheet pile edge for installation of drain tile and a pore pressure sensor next to the drain tile

A calibrated pore pressure sensor (Geokon Model 4500 vibrating wire) was installed next to the drain tile to monitor pore pressures after construction due to any water seepage into the backfill material. The sensor was embedded in a layer of sand that was bagged around the ceramic tip to prevent intrusion of fines.

Crushed limestone backfill material was placed in 6 in. lifts (after compaction) in the bottom 4 ft, and in 4 in. lifts above that (see Figure 10).

Figure 10. Placement of geosynthetic material and aggregate backfill material

A woven geotextile was installed between each layer and was wrapped around each layer against the sheet pile, to help avoid erosion of the backfill material.

A similar construction procedure was followed on the south abutment and the pore pressure sensor was installed next to the drain tile. The drain tile on the south abutment was about 1 ft below the elevation of the drain tile on the north abutment. The only difference on the south abutment was that a vertical sheet drain was installed against the face of the sheet pile wall, between the GRS backfill and the sheet pile.

The research team was not present during construction of the south facing, but the vertical sheet drain was reportedly wrapped around the drain tile near the bottom of the fill. The objective of the vertical sheet drain was to help improve backfill drainage during any future flood event. The sheet drain used at this site was a single-sided sheet drain with a molded core that functions as a flow channel and has a nonwoven geosynthetic filter fabric that prevents intrusion of fines. The sheet drain manufactured by NuDrain were used at this site.

2.4.2   Cast-On-Site Beam Construction

Figure 11 shows the bridge construction site after removal of the existing bridge.

Figure 11. Construction job site

At the time this image was captured, the new abutments and replacement box beams had not yet been constructed. The timber formwork used for beam fabrication is shown in Figure 12.

Figure 12. Steel reinforcing cage for beam

This figure also shows the top longitudinal and lateral reinforcement and lifting loops at the end in the bottom image. Note the series of longitudinal sonotubes that were used to create the internal voids.

One of the goals of this project was to construct the bridge without the use of a conventional crane. Along these lines, one of the original ideas for moving the beams in place was to use a large tow truck to "drag/launch" the beams into place. Given uncertainties about the practicality of this, a "test" beam was first constructed. This test beam was constructed following the original design plans and is the beam shown in Figure 12. Beams used in the actual bridge were constructed similarly, but did not include the internal voids.

For the test beam, strain gages were mounted on six different longitudinal bars, designated as 1 through 6 in Figure 13a.

STRAIN GAGE

1 2 3

4 5 6

DIRECTION OF PULL OUT OF PAGE
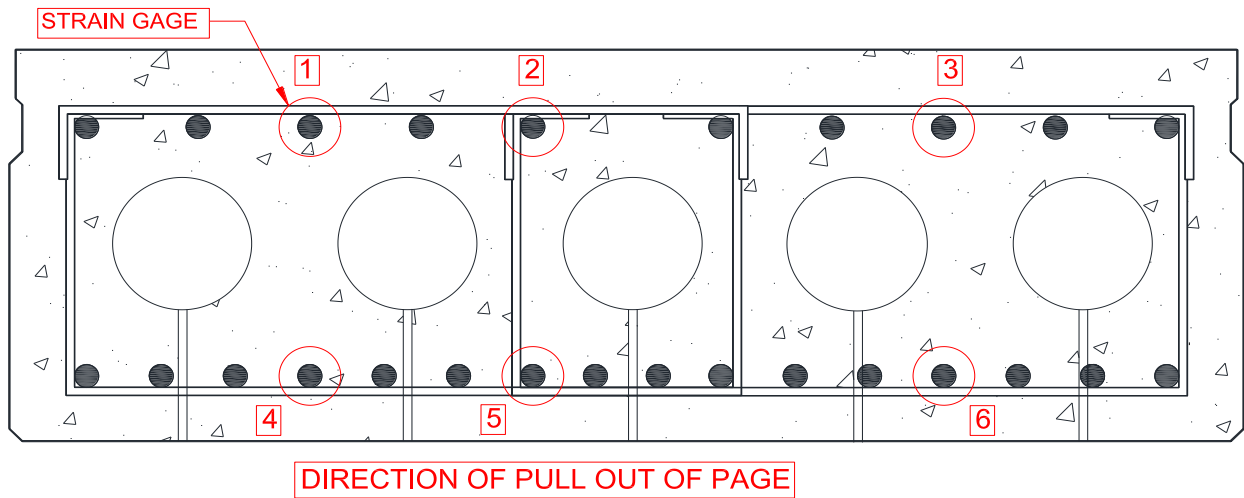
a**. Stain gage locations on longitudinal bars (at 1, 2, and 3, top, and 4, 5, and6, bottom) over a beam cross-section**

DIRECTION OF PULL
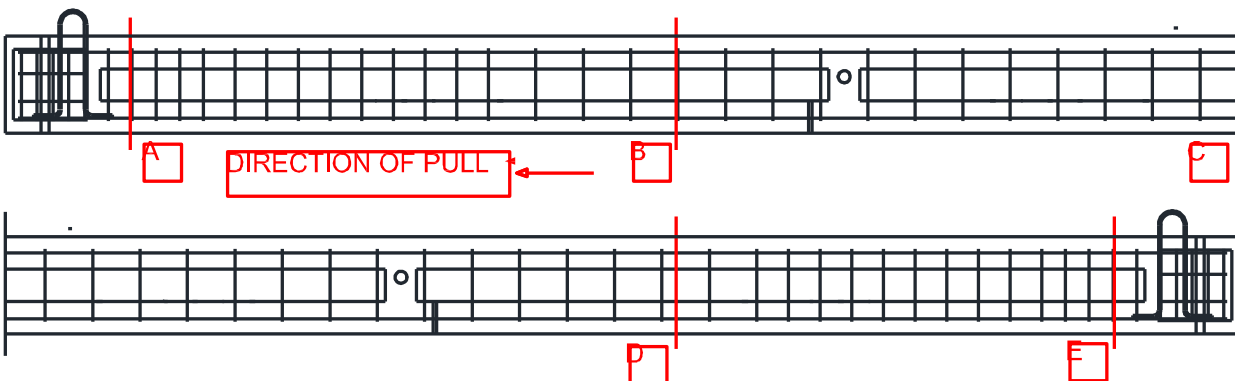
b. Strain gages at A, B, C, D, and E on longitudinal bars (top and bottom)

Figure 13. Internal instrumentation layout

Five cross-sections were instrumented with strain gages, labeled A through E in Figure 13b. Figure 14 shows a typical installation of a strain gage on the longitudinal reinforcement.

Figure 14. Gage installation on reinforcement

2.4.3   Tow Truck Lift/Pull

The first attempt to position a beam (the "test" beam) was with a tow truck. Figure 15 shows the horizontal pulling loops on the end of the beam, which were installed for this purpose.

Figure 15. Lifting/pulling setup

The beam was planned to be moved by putting treated poles (shown on top of the beam in Figure 15 and Figure 16) under the beam and sliding it over the timbers. Figure 16 shows the beam when it was lifted on one end.

a. Beam lifted by tow truck

b. The beam when one end was lifted by the tow truck

Figure 16. Beam lifted by the tow truck

The lifting was stopped at this point for observations. The lifting force was then gradually released to let the beam rest on the ground.

During the lift of the beam, three important observations were made. First, there was extreme bending of the pulling loops and a crack that propagated from the pulling loop, as shown in Figure 17.

Figure 17. Horizontal pulling loops after lift

Second, there was concrete spalling on the end opposite the pulling end of the beam as shown in Figure 18.

Figure 18. Concrete spalling on non-pulling end of the beam

Finally, although the tow truck could lift the beam vertically, it did not have sufficient capacity to "pull" the beam forward any appreciable distance. The design and construction teams found the use of a tow truck for this purpose to be unsuccessful.

2.4.4   Backhoe Lift/Move

Realizing that the tow truck method of construction was likely not going to be feasible, it was decided to maintain the spirit of the project by including construction equipment restrictions in the bridge plan set. Specifically, it was stated that the contractor could not use a conventional crane to place the bridge beams. No other restrictions were included.

The contractor selected for the project elected to use two backhoes to move the beams from their fabrication site to their final position on the bridge abutments. To document the behavior including peak behaviors, a series of externally mounted strain gages were installed on one beam prior to moving it. The external strain gages were mounted at three different cross-sections, one at 9 ft 8 in. from both the north and south ends and one at mid-span. The gage layout and the designations for those gages are shown in Figure 19.
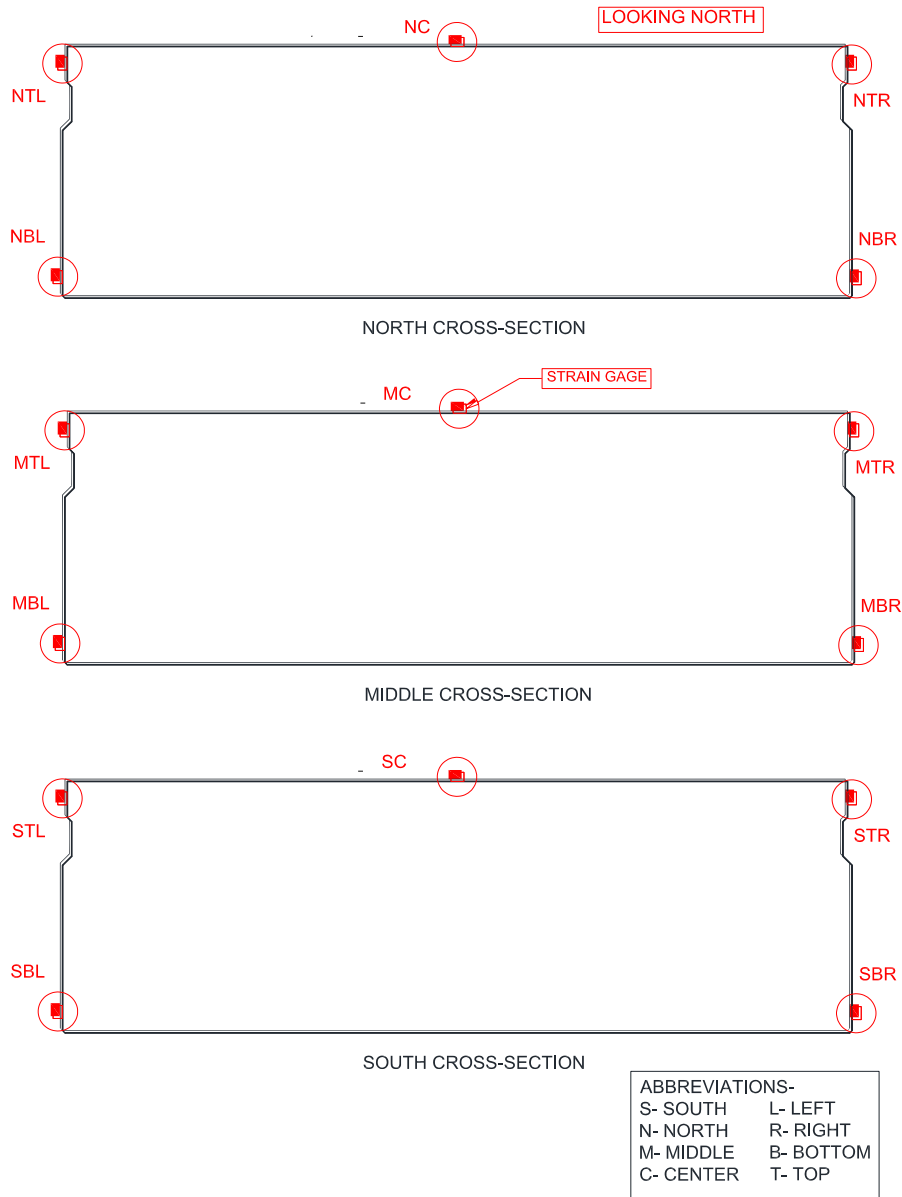
Figure 19. Strain gage layout for backhoe lift/move

All externally mounted gages had an effective gage length of 3 in. Figure 20 shows the strain gages mounted on the beam and data collection system that was used to record the strain during the beam move.

Figure 20. Installed strain gages and data collection system for lift/move

To facilitate placing the beams, a temporary bridge was constructed over the creek by placing steel girders across the creek and placing timber deck panels over the girders to make a traversable surface. As shown in Figure 21a, the two backhoes lifted the beam using preinstalled lifting loops.

| **a. Beam lift** | **b. Beam move over the creek** |

Figure 21. Beam launching using backhoes

After the beams were lifted, the backhoes moved the beams from where they were placed toward the creek by slowly tracking together in a coordinated fashion.

Figure 21b shows one backhoe crossing the creek over the temporary bridge.

Figure 22 shows four beams that had been placed on the concrete abutments while Figure 23 shows the fifth beam being moved to its designated location.

Figure 22. Four beams placed over the creek on the concrete abutments

Figure 23. Fifth beam being moved to its position using backhoe

The lifting loops were cut off 2 in. below the top surface of the beams and the recessed area was filled with a grout material. The keyway between adjacent beams was filled with non-shrink grout and cured following the manufacturer's recommendations. Backer rod was inserted along the bottom of the joint to seal the joint. Galvanized rods were used to complete the transverse tie

assembly. These 1 in. rods were tightened to a snug fit. Following tightening, the pockets that received the transverse tie bar on the outside were filled with grout.

3 BRIDGE EVALUATION

3.1 Tow Truck Pull/Lift-Test Results

During the lifting/pulling of the "test" beam attempt, internal strain data were recorded. Figure 24 shows the strains from the three internal gages on top at mid-span (i.e., C1, C2, and C3 in Figure 13).
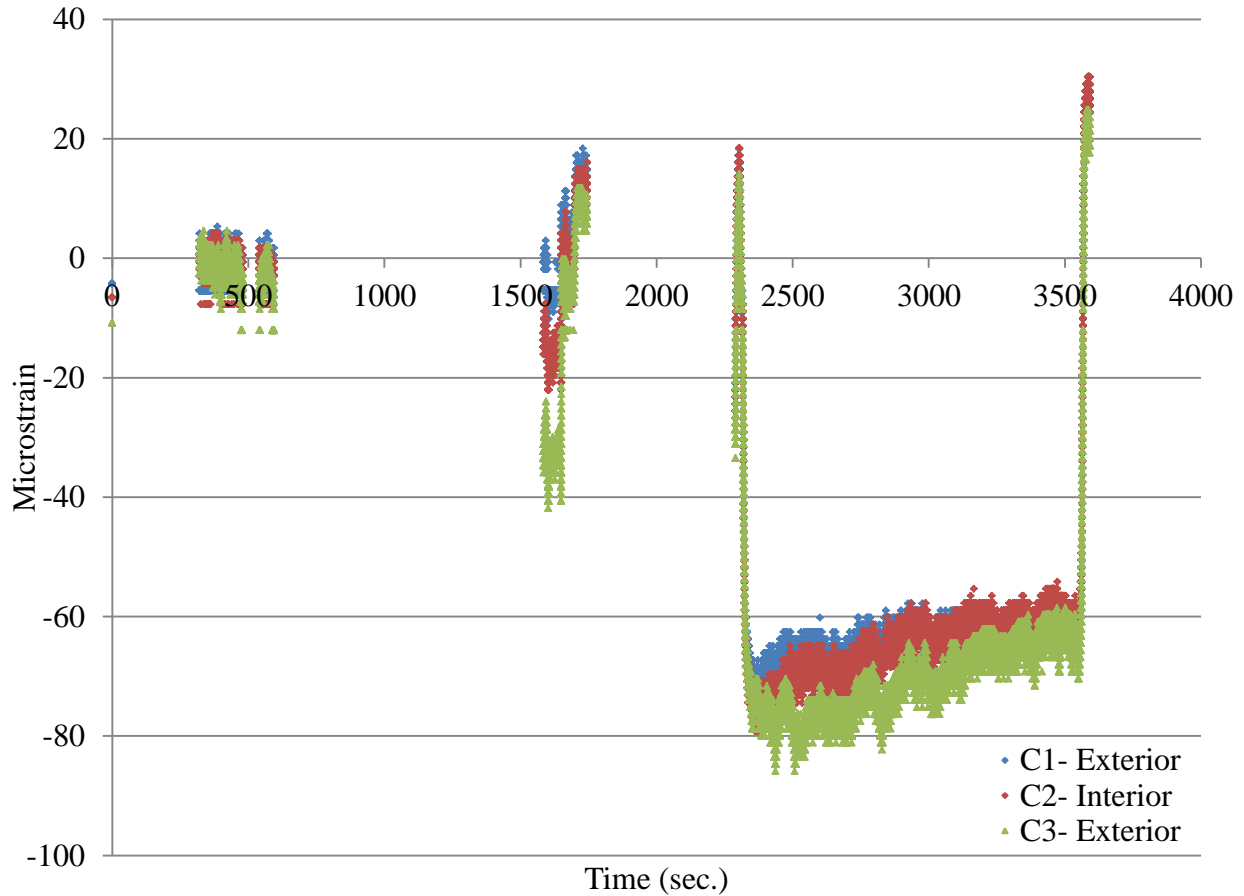
Figure 24. Typical top bar strain history (cross-section C top gages)

The microstrain values in Figure 24 are shown against time in seconds. Initially, an attempt was made to slide the beam without lifting it. However, while applying the pulling force, the front wheels of the tow truck lifted off the ground several inches. As a result, the pulling was stopped there. The strain values for this pull are shown around 500 sec. Another attempt was then made to pull the beam after the truck was positioned on more solid ground. This attempt also caused lifting of the front of the truck. This attempt was after 1,500 sec. (before 2,000 sec.) from the start of the test, as shown in the figure.

After the unsuccessful attempts at pulling the beam, it was decided to try to simply lift one end of the beam by applying a vertical force at one end. All three gages on top at mid-span reached

their peak values during this activity, which occurred between 2,000 and 4,000 seconds, as shown in Figure 24. Lifting of the beam resulted in positive bending (compression on top and tension on the bottom). Figure 25 shows the strain history of the bottom internal mid-span gage (C5 in Figure 13) with time.
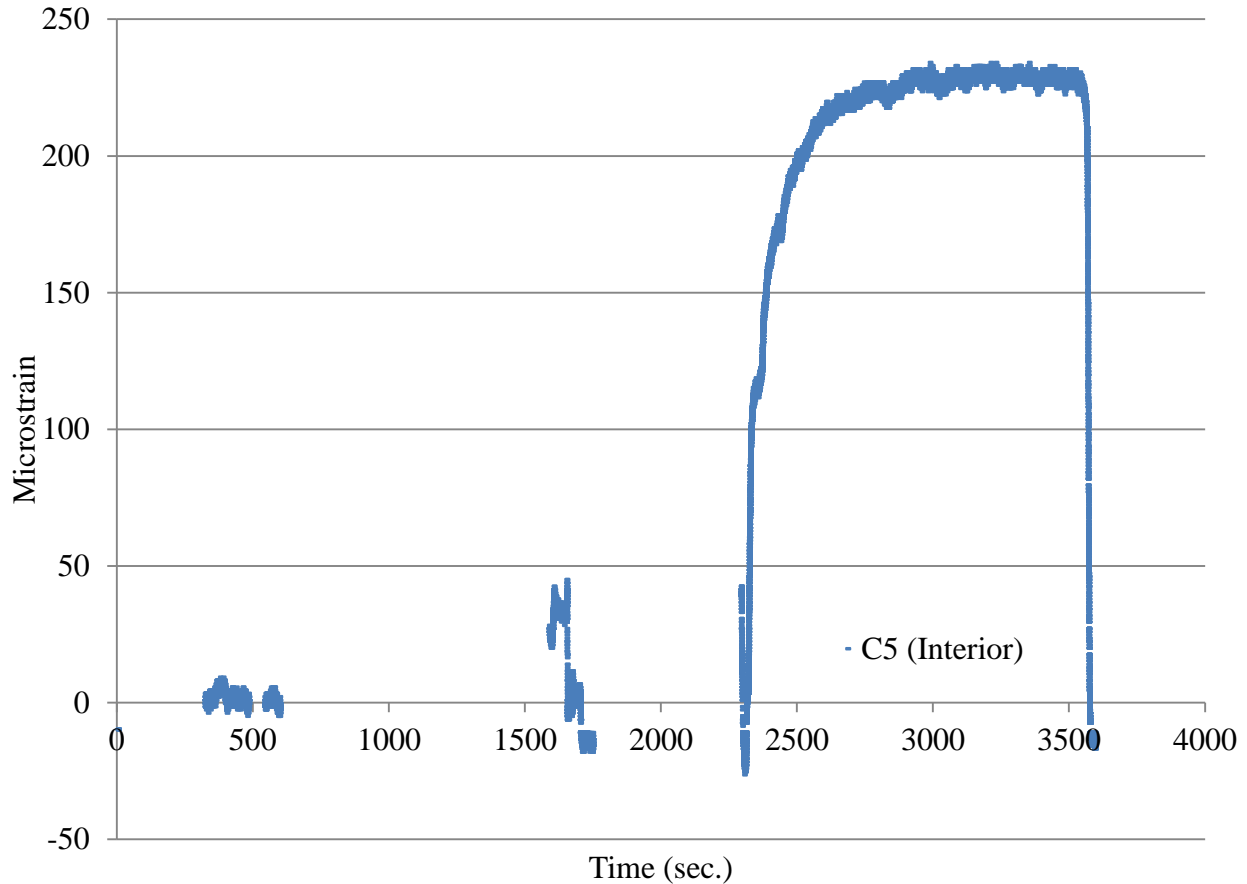
Figure 25. Typical bottom bar strain history (cross-section C bottom gage)

Similar to the top gages' history, the bottom gage reached peak strain values during the time when the beam was raised. Table 4 shows the peak strain values for the top three and bottom three longitudinal bars at each instrumentation cross-section (i.e., A through E in Figure 13b).

Table 4. Peak microstrain values in longitudinal bars

Bar	Location				
	A	**B**	**C**	**D**	**E**
Top	-35	-90	-80	-80	-30
Bottom	45	115	225	100	25

During the combined lifting/pulling attempts, a horizontal force was introduced into the beam that induced some additional tensile axial strain in the beam. This behavior resulted in larger tensile strains.

In addition to the instrumentation on the longitudinal bars, one strain gage was installed on top of each horizontal pulling loop. The peak value in this case was more than 10,000 microstrains due to the compression caused by the loop bending. Figure 26 shows the microstrain values over time for this gage.
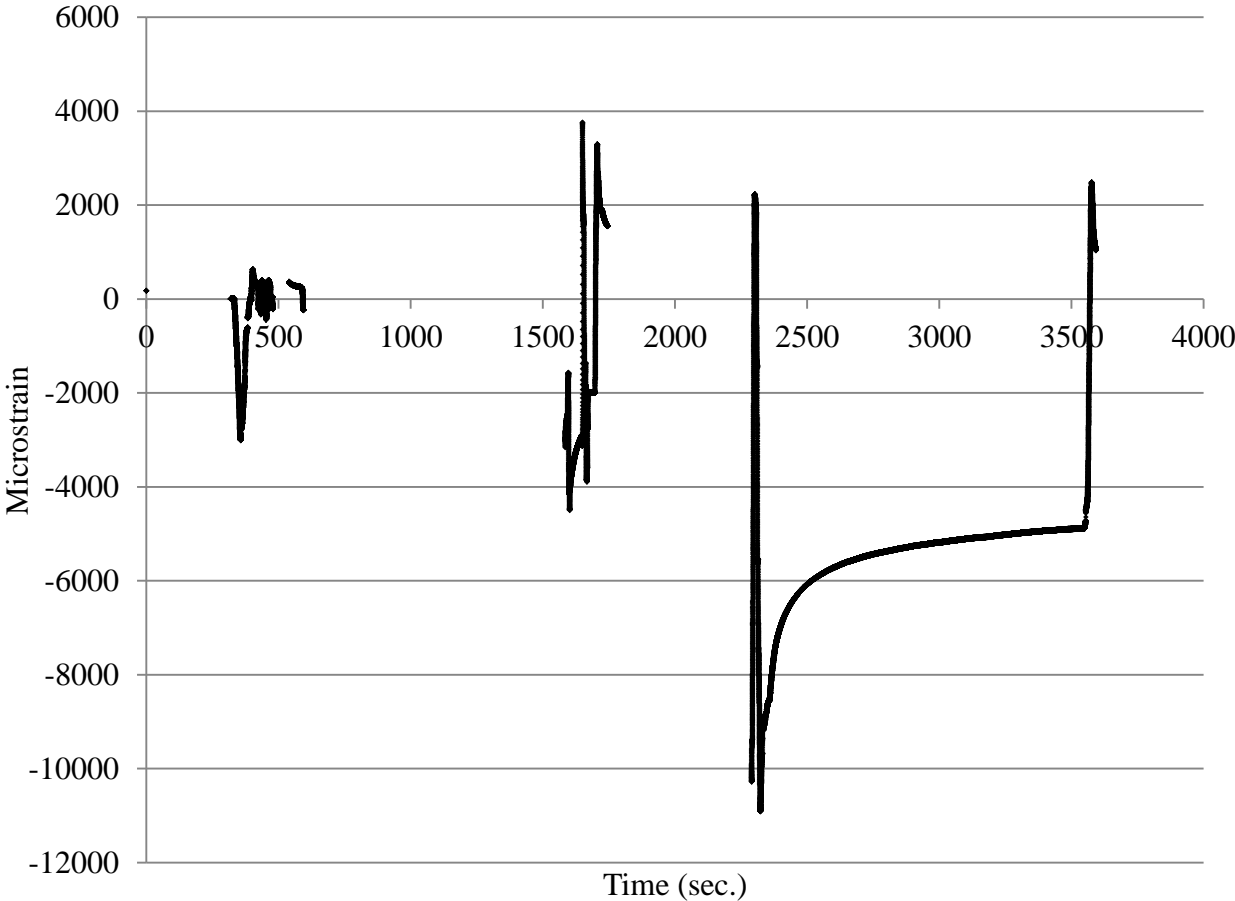
Figure 26. Horizontal pulling loop strain

As a result of the high strain in the lifting loops and the cracking and spalling of the concrete, coupled with the fact that the tow truck couldn't actually move the beam, hopes of using a tow truck to launch the beams seemed unlikely. However, as mentioned previously the spirit of the project was maintained by restricting the types of heavy construction equipment that could be used to construct the actual bridge. Specifically, it was envisioned that a county or small bridge contractor might not have a high capacity vertical crane available to place the beams. And, given that the intent of this project was to demonstrate a bridge system that could be constructed by county workforces, it was decided that the means and methods used to place the beams be determined by the bridge contractor.

3.2   Backhoe Lift/Move-Test Results

As previously mentioned, the contractor elected to use a pair of backhoes to lift, move, and place the bridge beams. Figure 27 shows the strain history for the external south cross-section gages (shown in Figure 19) during this process.
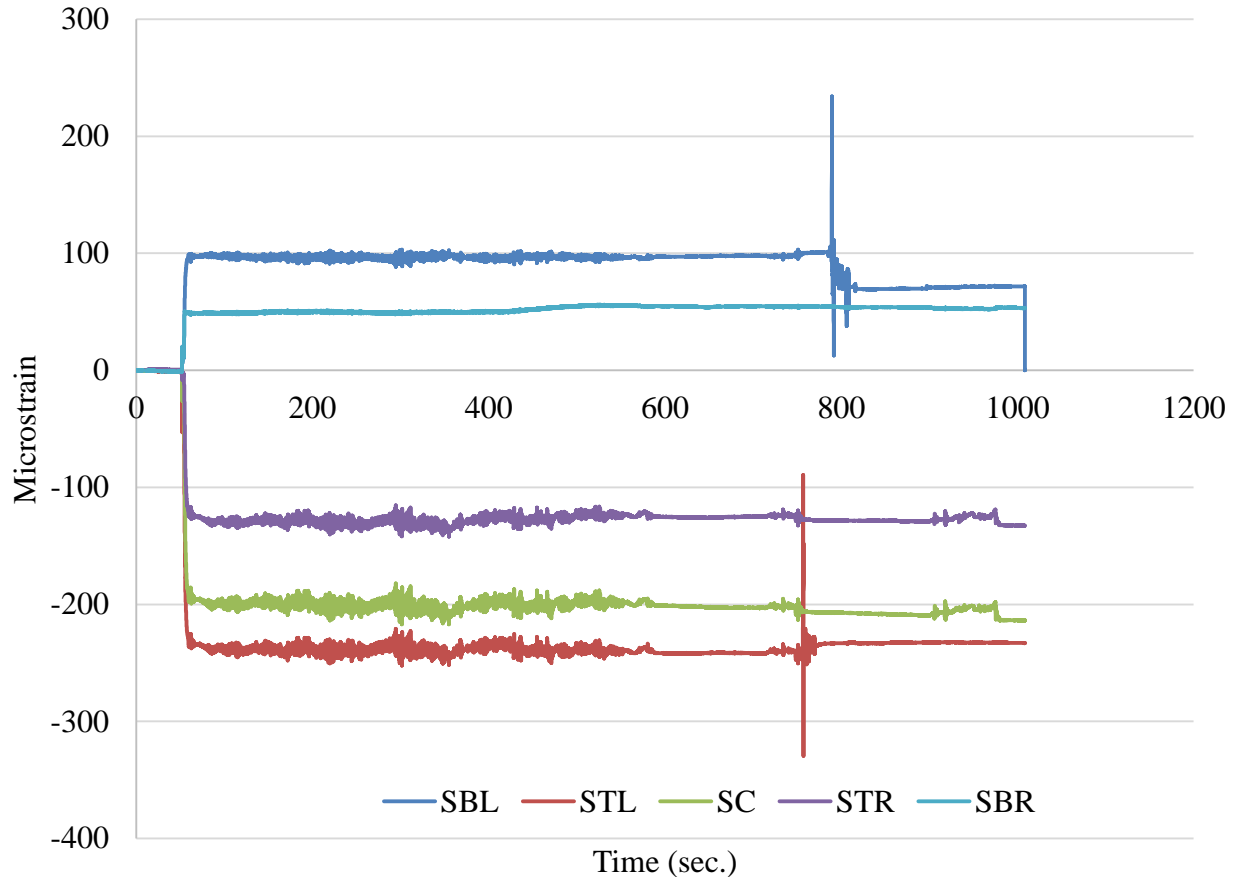
Figure 27. Strain history for south cross-section

As Figure 27 shows, the beam was placed into positive bending when initially lifted and that, for the majority of the process, the strain magnitudes remained relatively constant. However, at just before 800 seconds following data collection initiation, a rapid strain change occurred.

Figure 28 and Figure 29 show the strain history for the north and middle cross-sections, respectively.
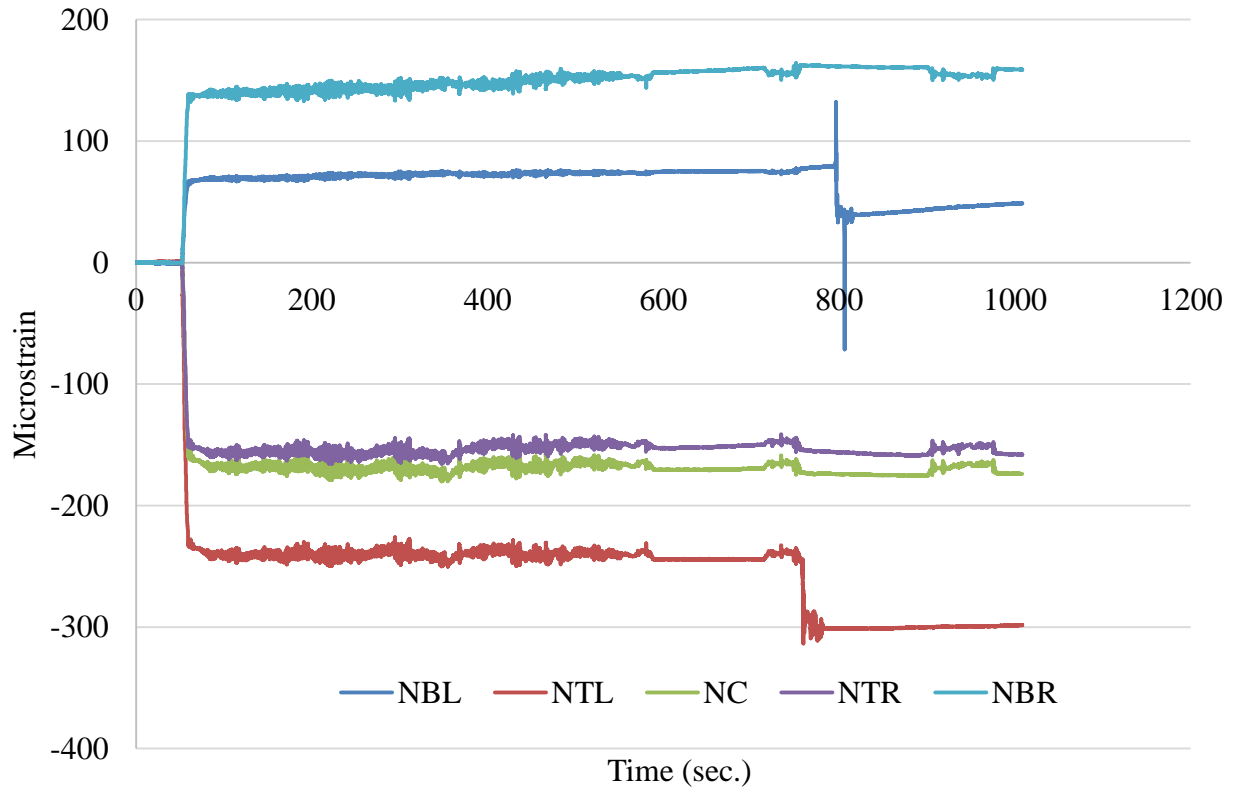
Figure 28. Strain history for north cross-section
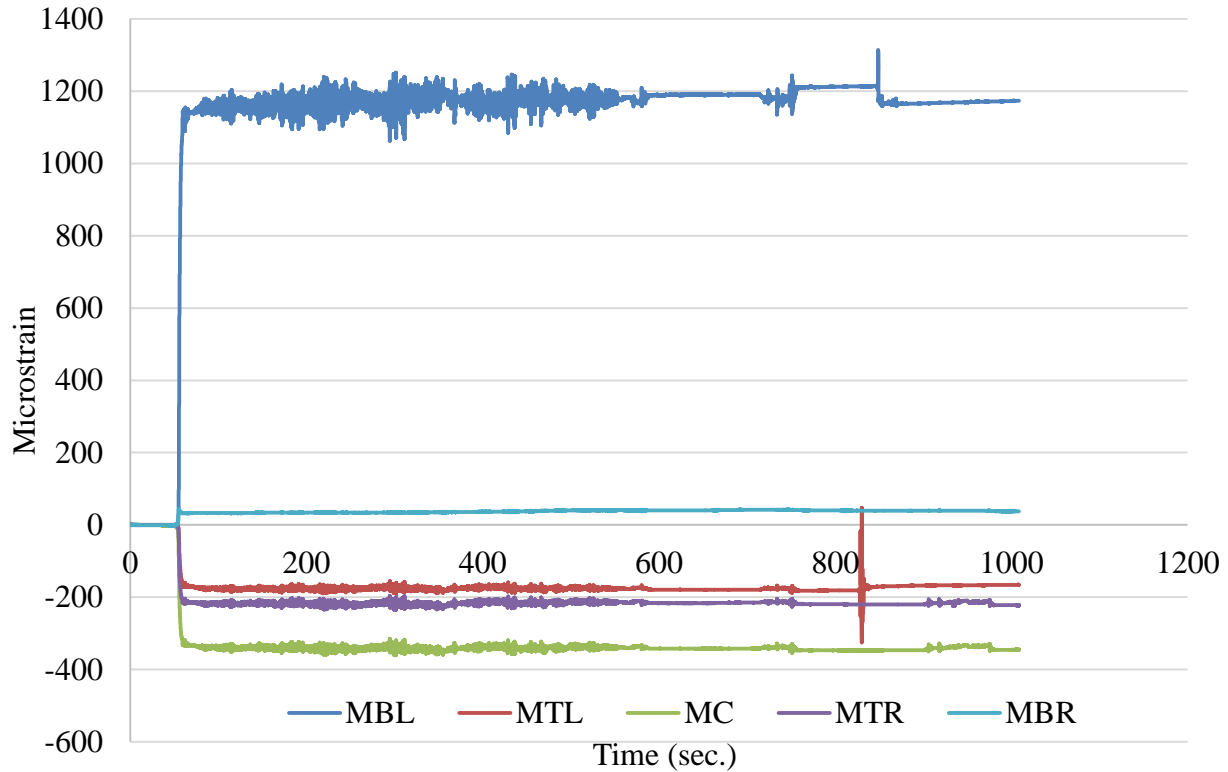
Figure 29. Strain history for middle cross-section

The strain history for the north cross-section is similar to the south cross-section. An almost constant behavior can be observed at all locations throughout the entire lift, move, and place process. Of particular interest is the measured behavior of the middle cross-section in Figure 29, which shows peak values for tension up to 1,200 microstrains for the gage MBL, which is much higher than the other cross-section locations and highly indicative of the development of cracks on the bottom surface of the beam.

3.3   Live Load Testing

After construction of the bridge, live load testing of was carried out, annually, for three consecutive years (2014, 2015 and 2016). For the load tests, the bridge beams were instrumented with externally mounted strain gages. Following instrument installation, a loaded truck was driven over the bridge while recording the data from the gages. Figure 30 shows the different load cases that were used for the tests.
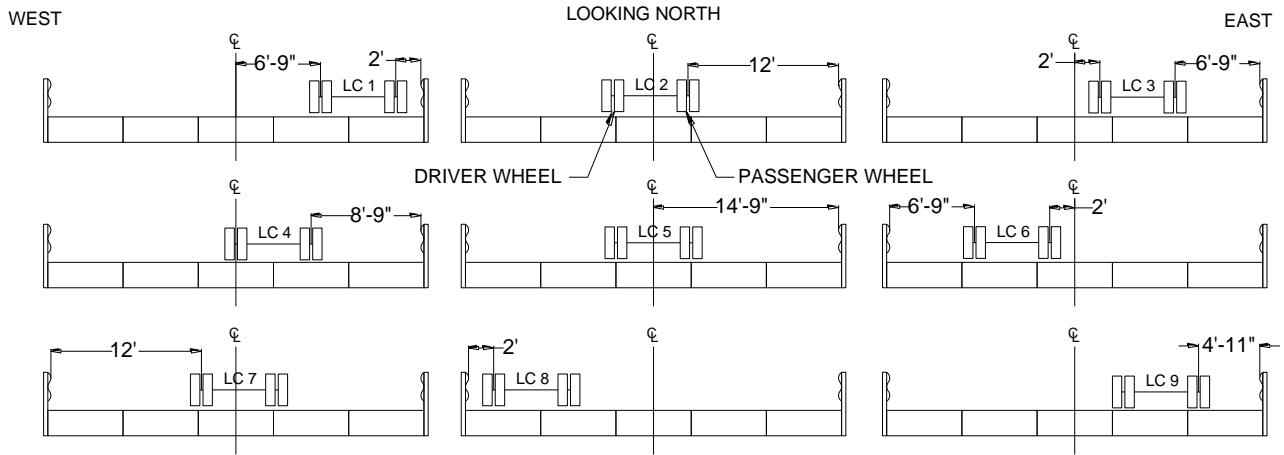
Figure 30. Load cases

In this figure, the transverse location of the truck is shown. Gages were installed on the beams to record the longitudinal strain in the beams and deflection transducers were installed to measure the relative displacement between adjacent beams. Figure 31 shows the instrumentation layout and nomenclature.
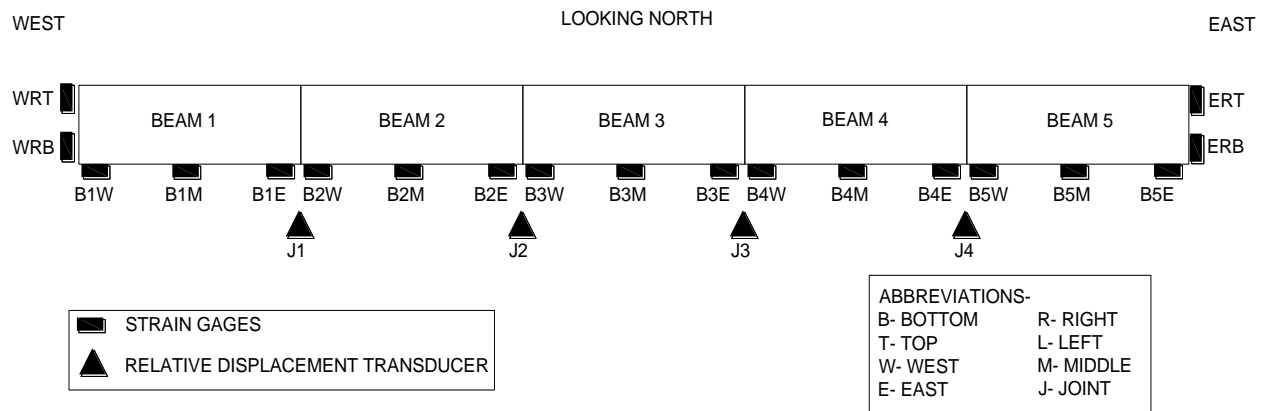
Figure 31. Instrumentation layout and nomenclature

Figure 32 shows the bridge after all external instrumentation was installed. Figure 33 shows a close-up view of the relative displacement gage setup that was used to monitor for relative moment between adjacent beams.

Figure 32. Instrumentation mounted on the bridge

Figure 33. Relative displacement gage setup

Figure 34 shows the loaded tandem-axle dump truck being guided across the bridge in a pre-designated position. For each load case, the truck was slowly driven (approximately 3 mph) from one end to other while keeping the truck in a consistent transverse position.

Figure 34. Live load testing on the bridge

3.3.1   Load Test Results

In general, the strain history from the load tests from all three years showed a similar pattern. To simplify the analysis, the test results were normalized to the weight of the truck used for the first load test (gross weight of 52,360 lbs).

Figure 35 shows the strain distribution for Load Case 1 (LC-1) for all three years.
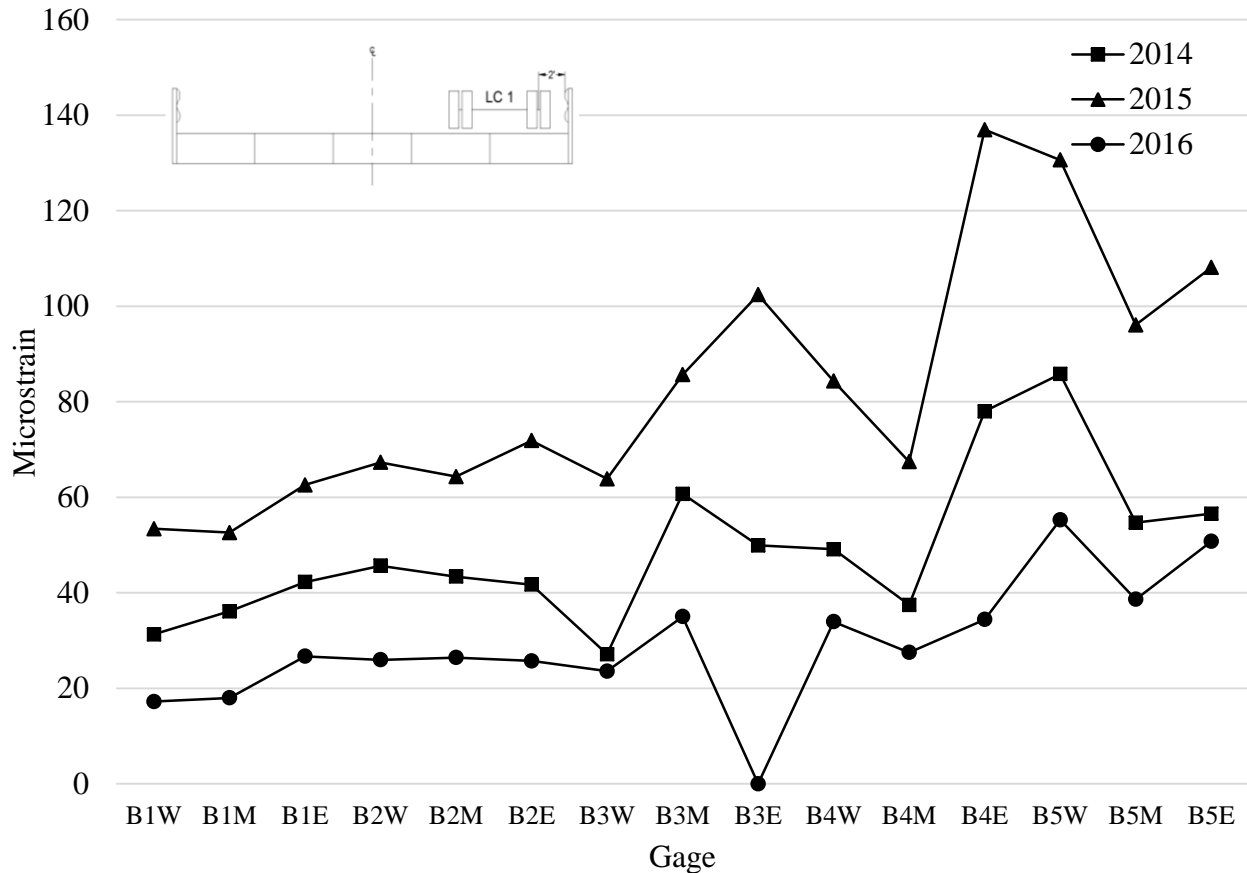
Figure 35. Longitudinal strain distribution over the transverse mid-span (LC-1)

The x-axis on the graph represents the strain gages from left (west) to right (east) when looking north. This figure shows the higher level of strains near the truck wheel locations. The B3E gage for year 2016 malfunctioned. The peak value in this case was 140 microstrains for year 2015, which is close to the tensile cracking strain of the concrete, indicating that there could have been a new or preexisting crack under the strain gage.

Figure 36 shows the strain distribution at mid-span for LC-5, when the truck is centered laterally on the bridge.

36
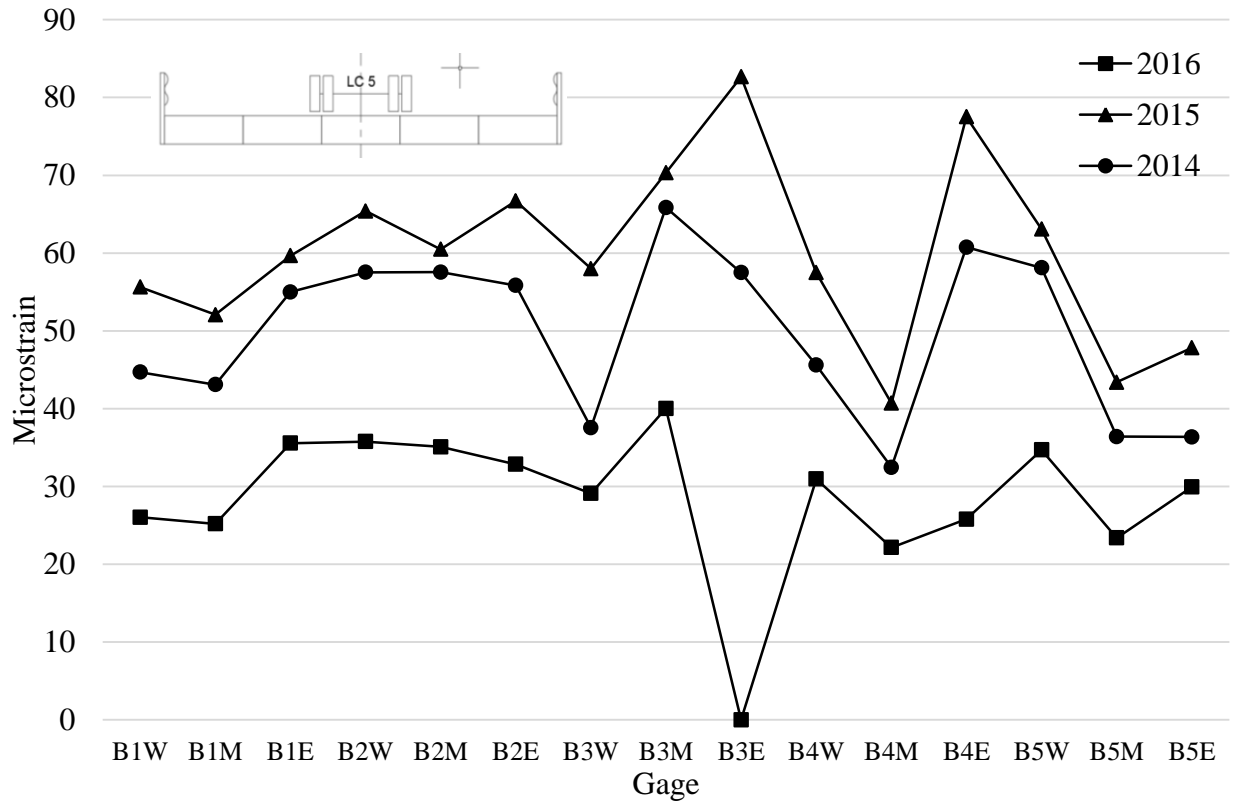
Figure 36. Longitudinal strain distribution over the transverse mid-span (LC-5)

Similar to LC-1, the strain values under the truck location are higher compared to the other locations. The measured strains with the truck in this position are, as expected, lower than when the truck was not centrally placed, with the highest strain value measured at about 83 microstrains in 2015.

Figure 37 shows the strain distribution at mid-span for LC-8 when the truck was driven very close to the west curb. The peak strain value in this case was 90 microstrains.
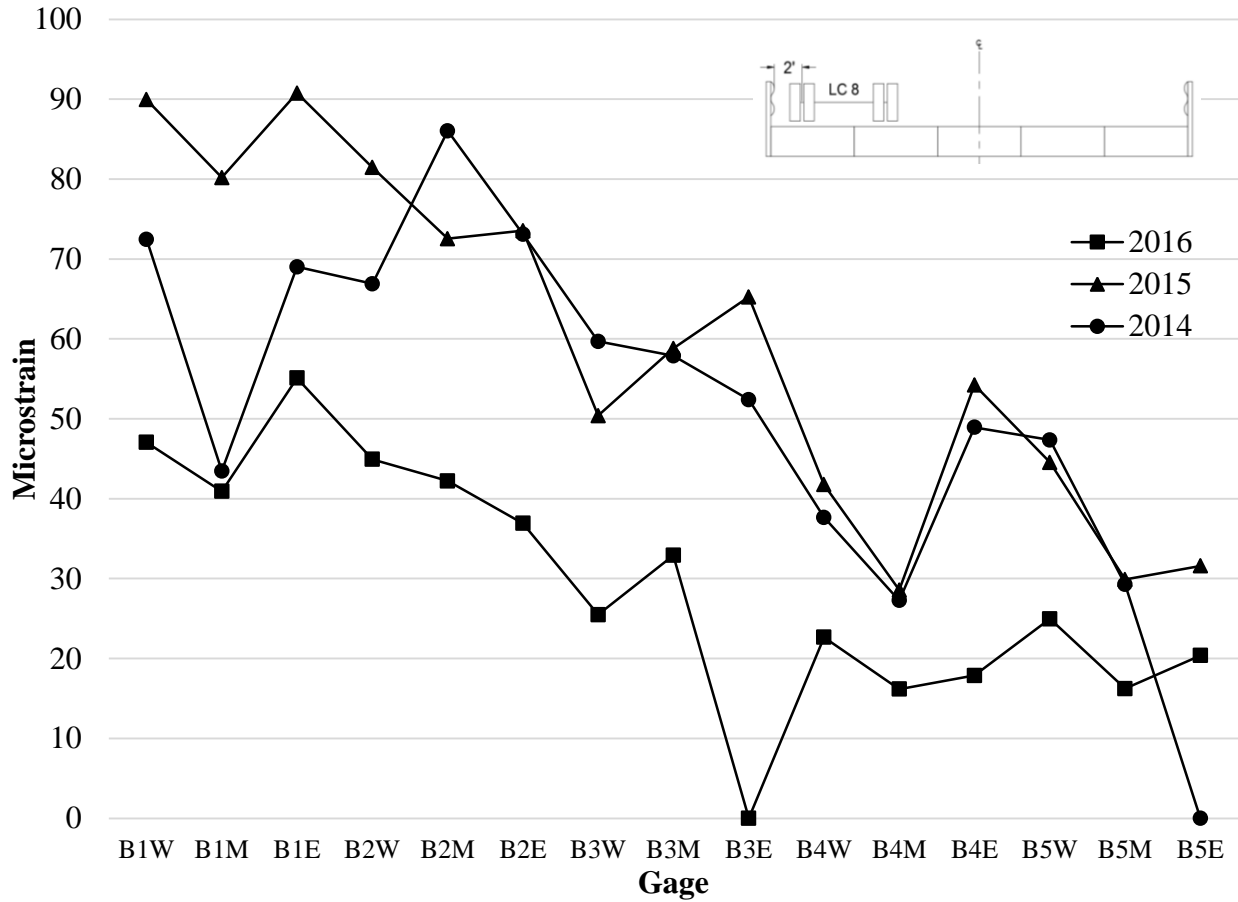
Figure 37. Longitudinal strain distribution over the transverse mid-span (LC-8)

Figure 38 shows the history of strain gages B1E and B2W mounted near Joint J1 for LC-6. The peak strain value is reached when the truck is above the strain gages, i.e., mid-span.
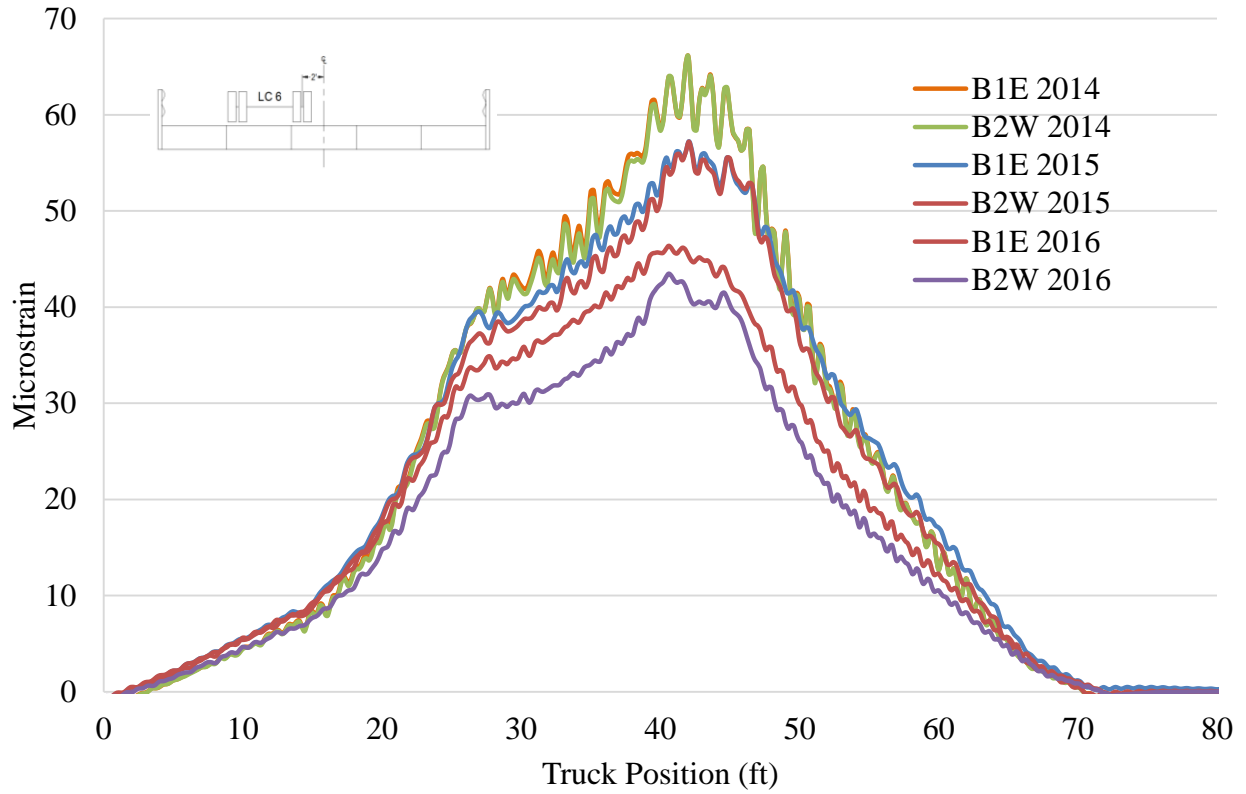
Figure 38. History of the strain gages near Joint J1 (LC-6)

Figure 39 shows the history of strain gages B4E and B5W mounted near Joint J4 for LC-3.
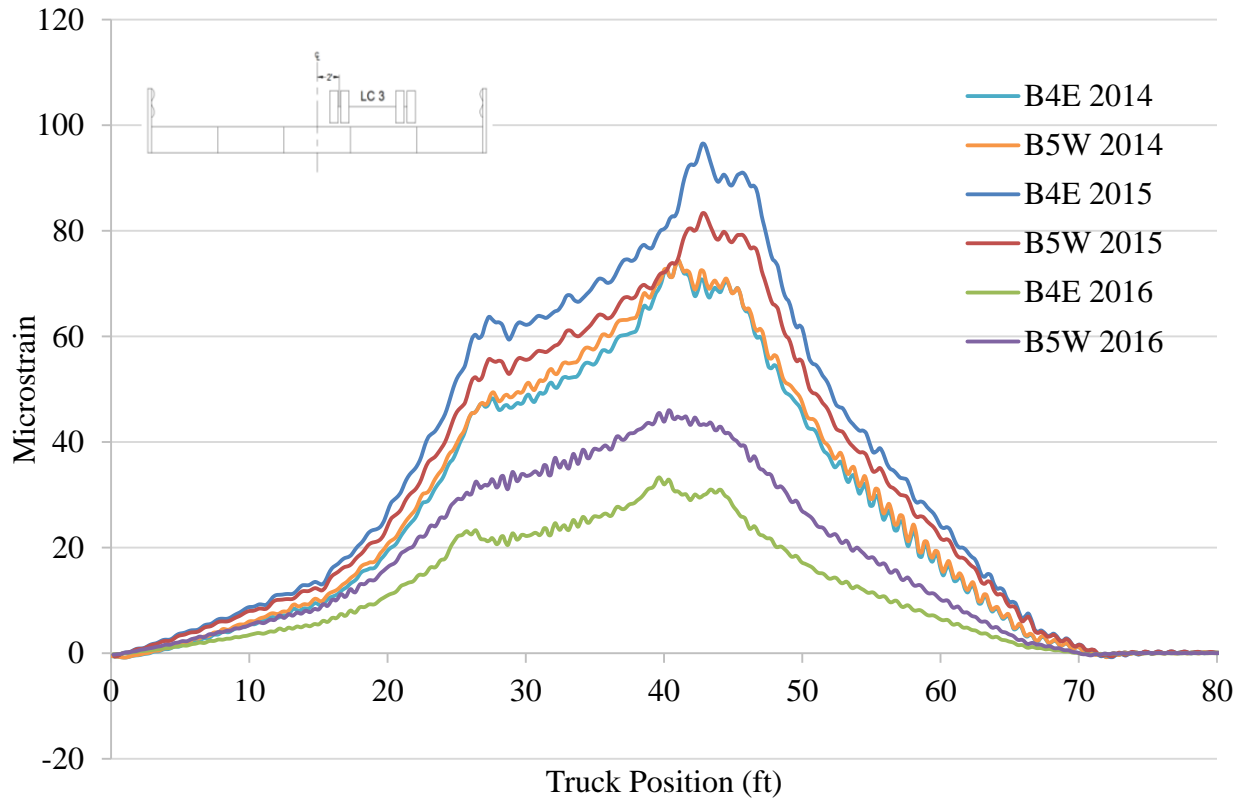
Figure 39. History of the strain gages near Joint J4 (LC-3)

Similar to the case of J1, LC-3 was used to determine peak strains for J4. From the strain history for these gages in Figure 38 and Figure 39, there is no significant difference in strain values and the peak strain values are low.

Figure 40 shows the history of relative displacement between Beam 1 and Beam 2 at Joint J1 for LC-6 for all three years.
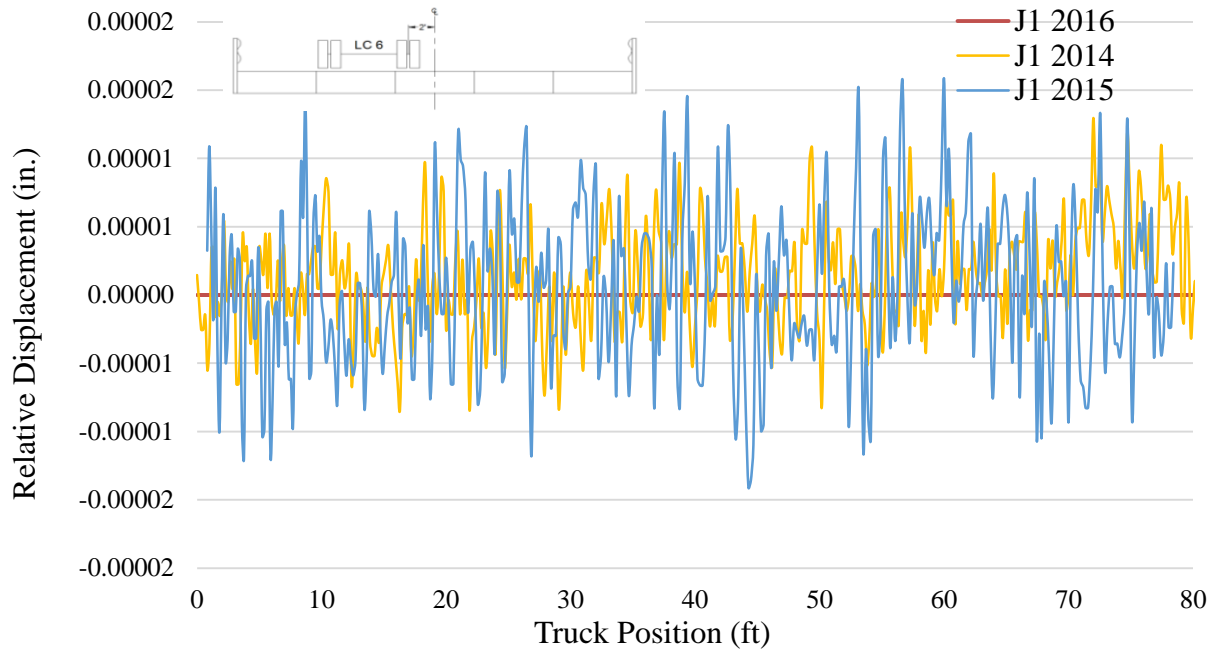
Figure 40. History of relative displacement at Joint J1 (LC-6)

From this history, it can be seen that, the relative displacement transducer for the year 2016 failed. The peak relative displacement value was about 0.00002 in., which is small.

Similarly, Figure 41, Figure 42, and Figure 43 show the relative displacement at the joints J2 (LC-6), J3 (LC-9), and J4 (LC-3) respectively.
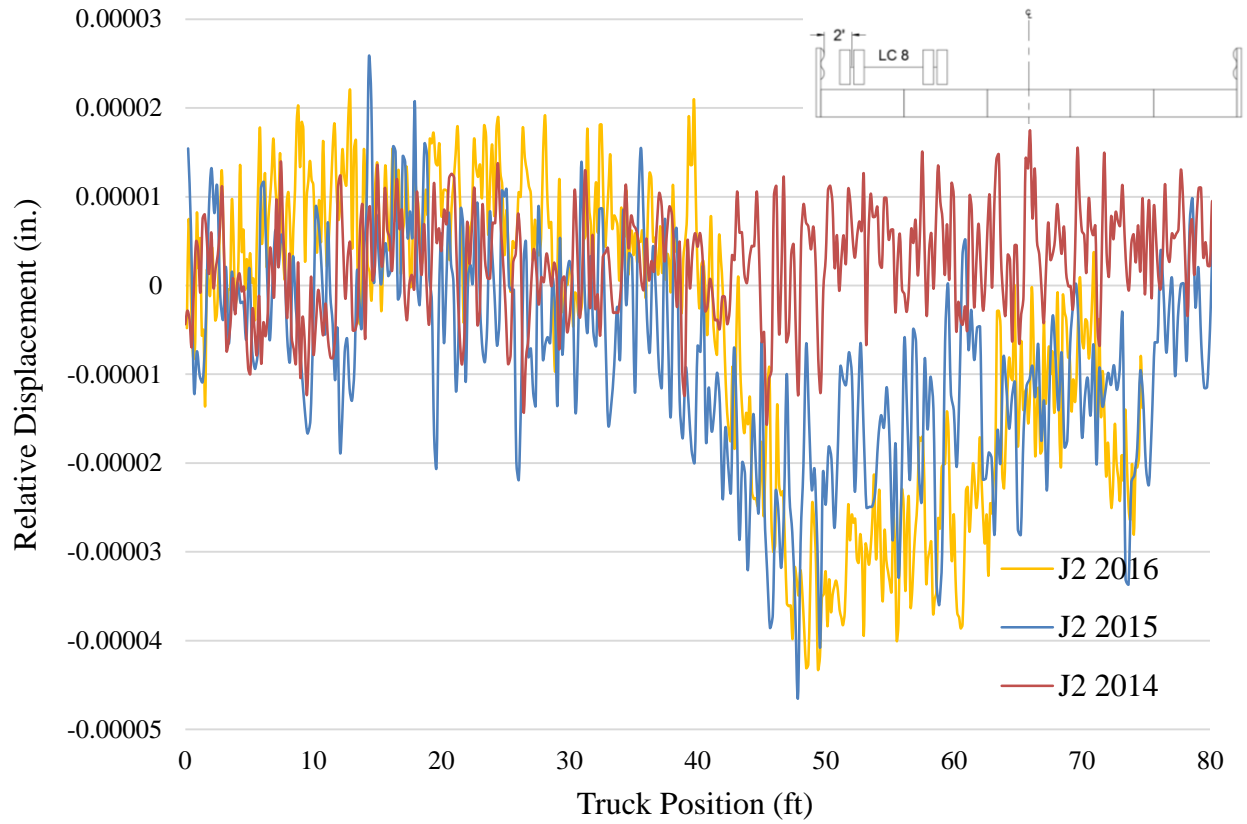
Figure 41. History of relative displacement at Joint J2 (LC-8)
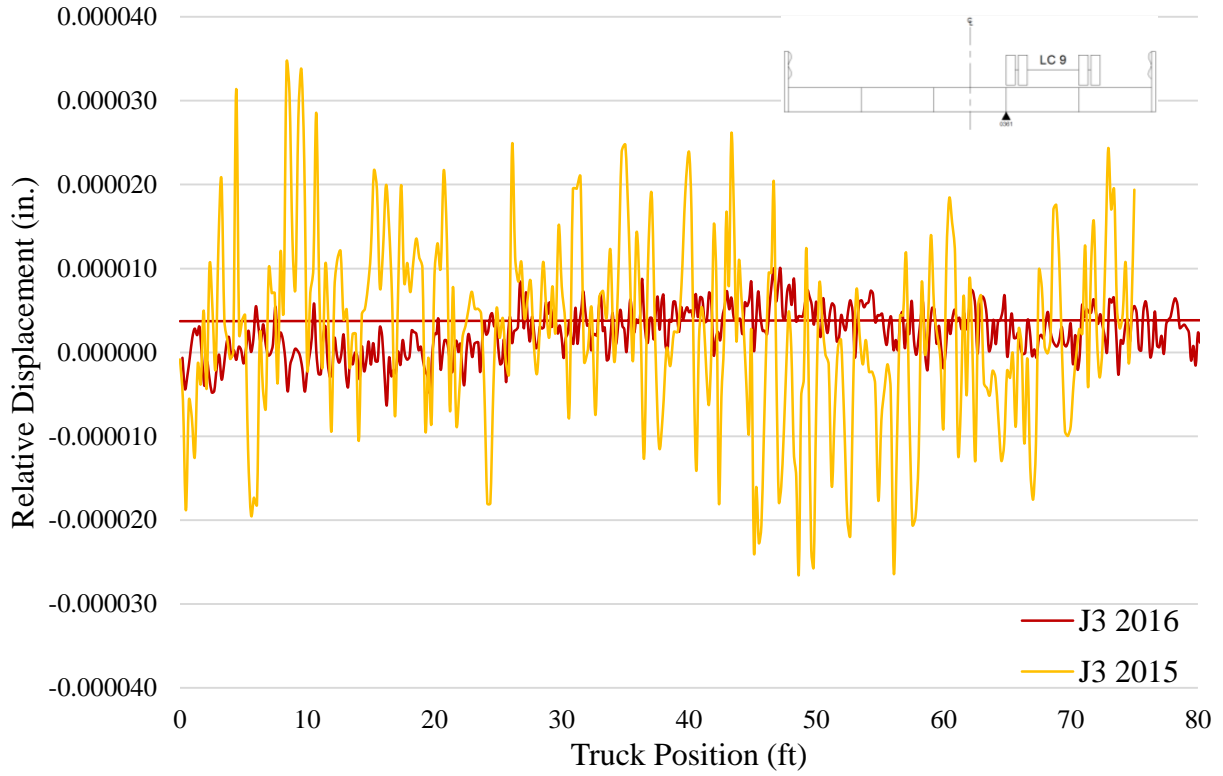
Figure 42. History of relative displacement at Joint J3 (LC-9)
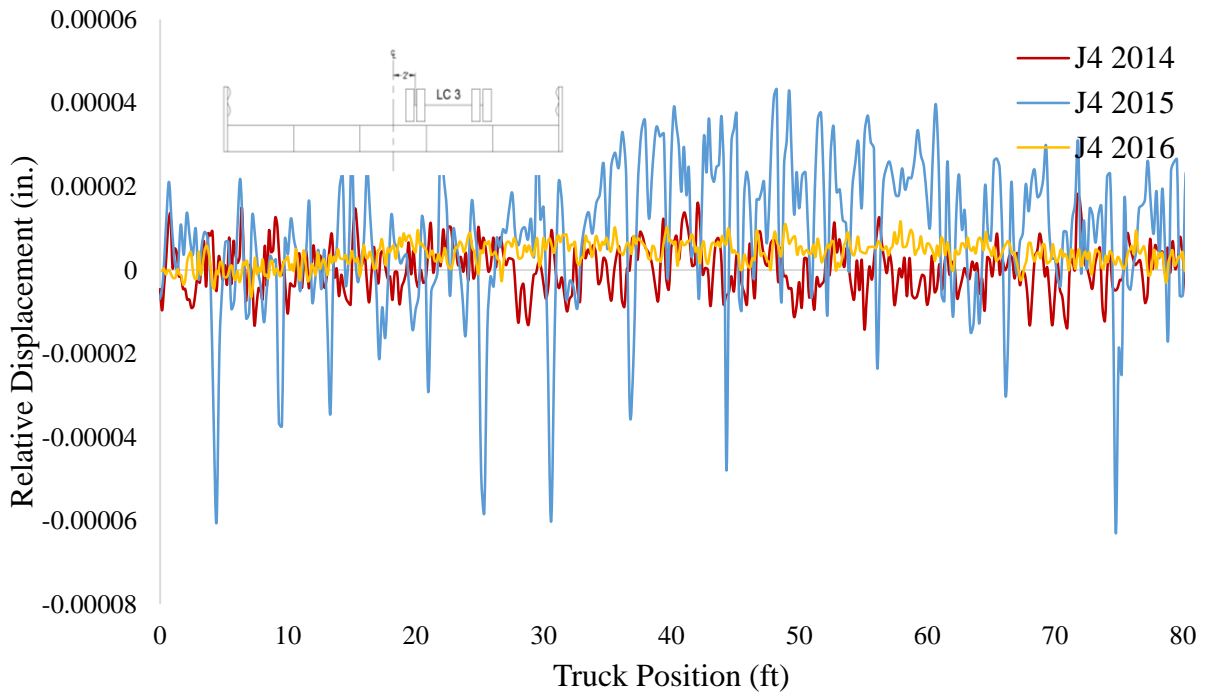
Figure 43. History of relative displacement at Joint J4 (LC-3)

43

These figures show the various patterns recorded by the relative displacement transducers. The highest relative displacement was -0.0004 for Joint J3 (LC-9) for the year 2014. The year 2016 load test had the smallest relative displacement. Relative displacement history of Joint J3 for year 2014 is not shown because the transducer malfunctioned.

3.3.2 Load Distribution Factors

The load distribution characteristics of the bridge were investigated by comparing the calculated distribution factors from the measured strains with those calculated using American Association of State Highway and Transportation Officials (AASHTO) LRFD specifications (2012).

Figure 30 showed that some of the load cases were similar to each other, i.e. LC-1 and LC-9 were similar, LC-3 and LC-4 were similar, and LC-2, LC-5, and LC-7 were similar. Only one load case for each similar set was used for calculation. Distribution factors were calculated based on the assumption that the box beams have equal stiffness; the effect of guardrails on exterior beam (Beam 1 and Beam 5) stiffnesses was not taken into account. Based on this assumption, distribution factors for box beams can be calculated using the following equation:

$$DFi = \frac{\varepsilon i}{\sum_{i=1}^{n} \varepsilon i} \tag{4}$$

where DFi = distribution factor for the ith box beam, εi = strain measured in the ith box beam, $\Sigma \varepsilon i$ = sum of all box beam strains for a particular load case, and n = number box beams in the bridge.

For the calculation of distribution factors, the strain in the middle gage of each beam was used (gages shown in Figure 31). The AASHTO-specified load distribution factor was calculated using section 4.6.2.2.2 (AASHTO 2012). The calculated value of the load distribution factor according to AASHTO was 0.5. Table 5, Table 6, and Table 7 show the calculated values for the box beam load distribution factors for 2014, 2015, and 2016, respectively.

Table 5. Calculated box beam load distribution factors for 2014

Load Case	Beam 1	Beam 2	Beam 3	Beam 4	Beam 5
LC-1	0.16	0.19	0.26	0.16	0.24
LC-3	0.17	0.21	0.28	0.16	0.20
LC-5	0.18	0.24	0.28	0.14	0.15
LC-6	0.18	0.31	0.26	0.12	0.13
LC-8	0.18	0.35	0.24	0.11	0.12

Table 6. Calculated box beam load distribution factors for 2015

Load Case	Beam 1	Beam 2	Beam 3	Beam 4	Beam 5
LC-1	0.14	0.18	0.23	0.18	0.26
LC-3	0.16	0.19	0.25	0.18	0.22
LC-5	0.20	0.23	0.26	0.15	0.16
LC-6	0.25	0.26	0.24	0.12	0.13
LC-8	0.30	0.27	0.22	0.11	0.11

Table 7. Calculated box beam load distribution factors for 2016

Load Case	Beam 1	Beam 2	Beam 3	Beam 4	Beam 5
LC-1	0.12	0.18	0.24	0.19	0.27
LC-3	0.14	0.20	0.26	0.18	0.21
LC-5	0.17	0.24	0.27	0.15	0.16
LC-6	0.22	0.27	0.25	0.12	0.13
LC-8	0.28	0.28	0.22	0.11	0.11

Figure 44 through Figure 48 show the three-year experimental versus AASHTO-specified load distribution factors for LC-1, LC-3, LC-5, LC-6, and LC-8, respectively.
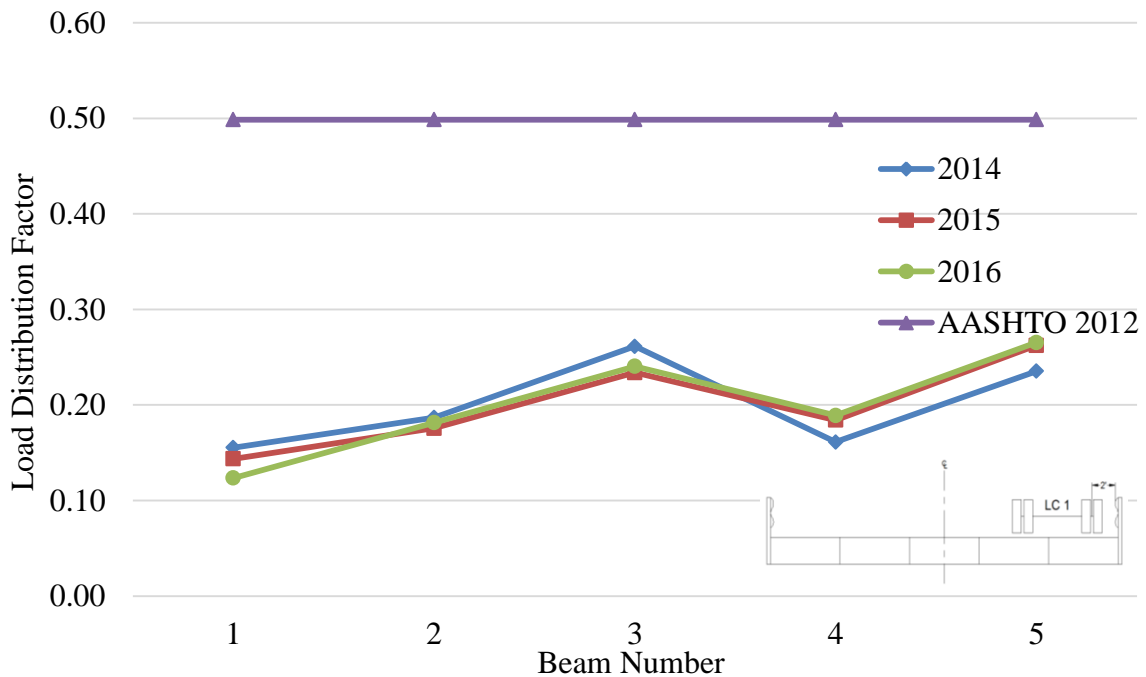
Figure 44. Experimental and AASHTO-specified load distribution factors for LC-1
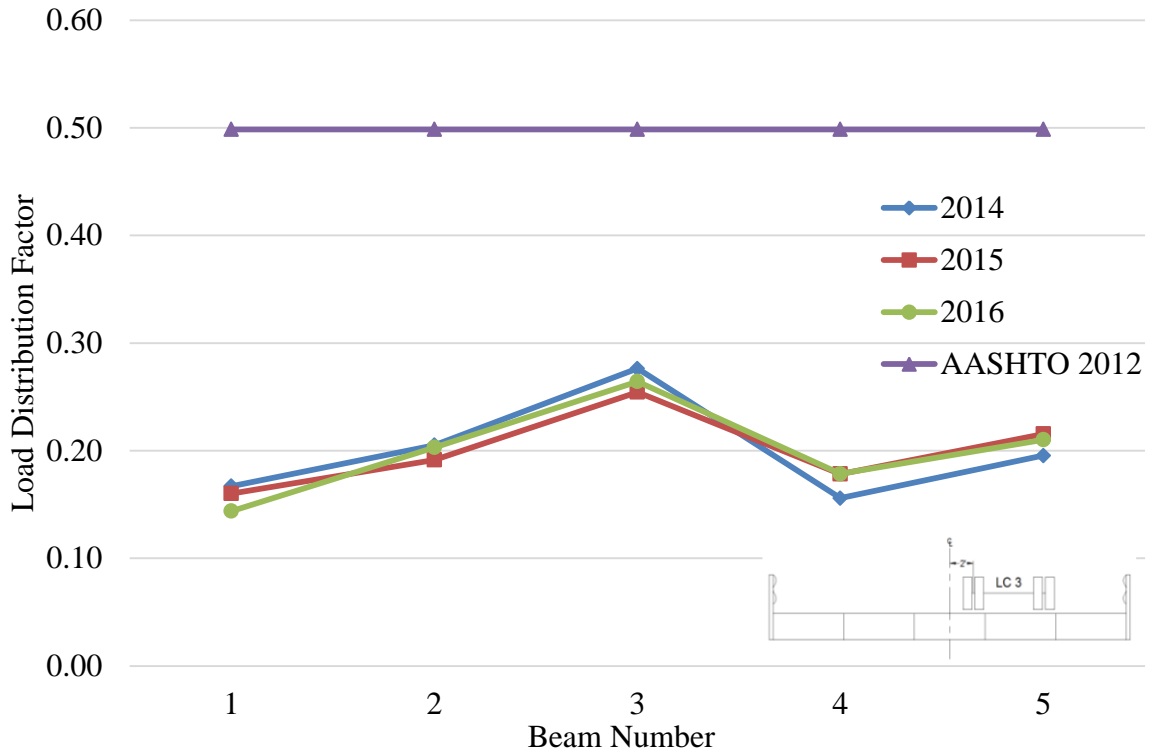
Figure 45. Experimental and AASHTO-specified load distribution factors for LC-3
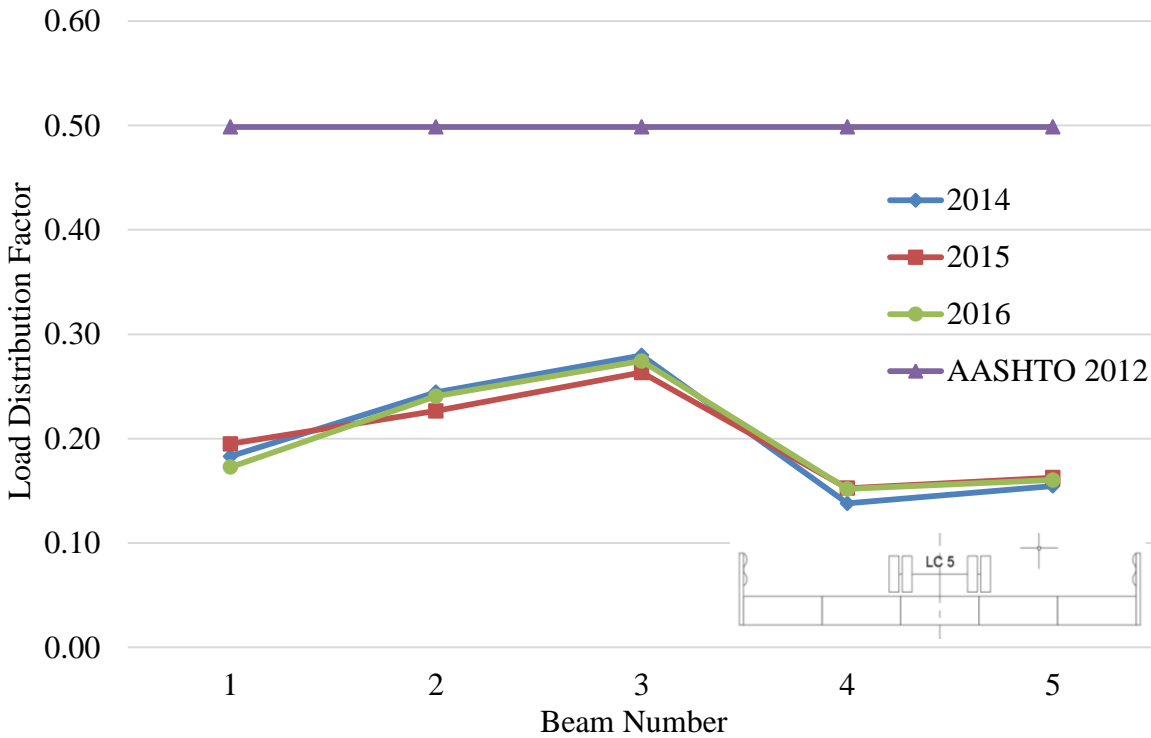
Figure 46. Experimental and AASHTO-specified load distribution factors for LC-5
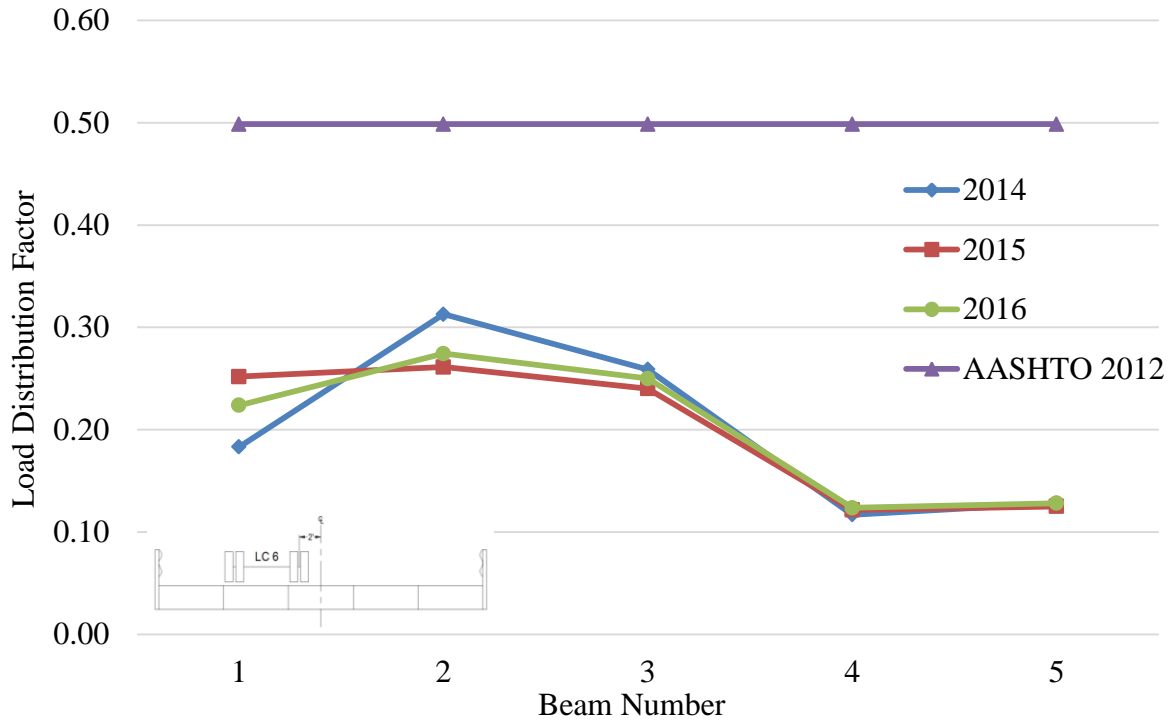
Figure 47. Experimental and AASHTO-specified load distribution factors for LC-6
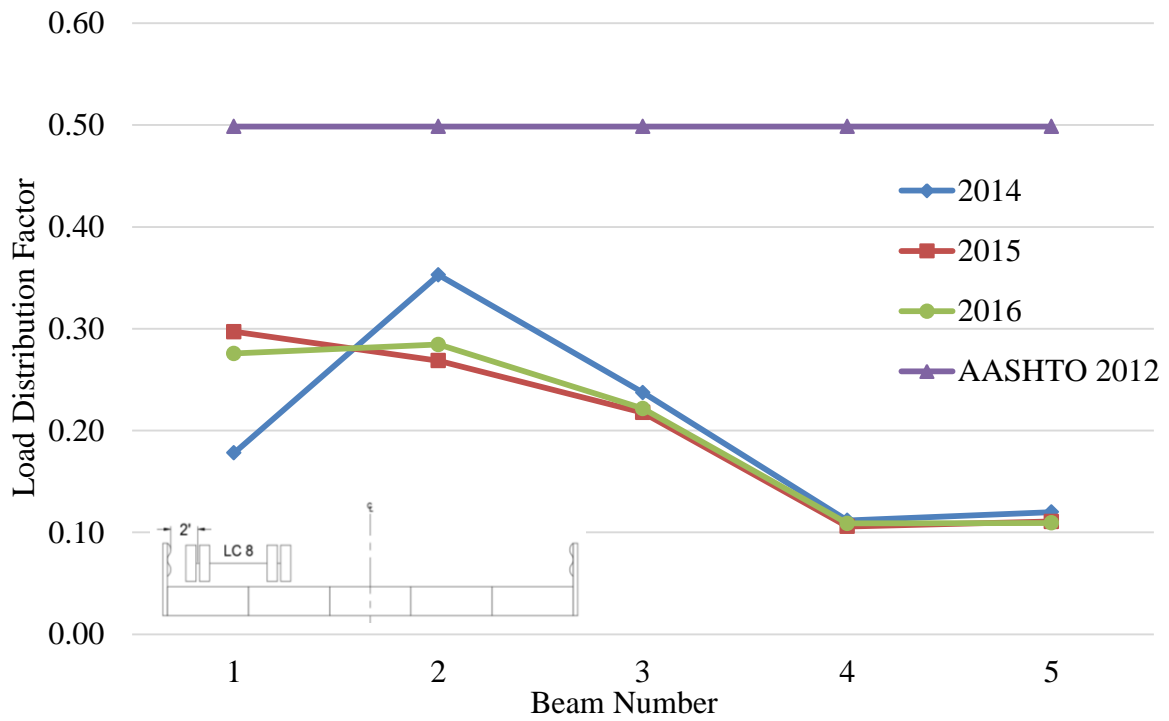
Figure 48. Experimental and AASHTO-specified load distribution factors for LC-8

From these figures, two things are noticeable. The load distribution factors show similar pattern over the three years for each load case and all the experimental distribution factors fall below the code specified value.

3.4   GRS Abutment Evaluation

Previous evaluations of GRS abutments in Buchanan County focused on the stress distributions under loading and stability of the abutment after flood events (Vennapusa et al. 2012). GRS abutments have shown excellent results in terms of load bearing capacity and stability. In this project, the primary focus of monitoring was to assess if there would be any advantage to using the sheet drain, which provides active vertical drainage, to help improve drainage in the GRS backfill during a flood event.

Pore water pressure in both abutments were monitored from October 2014 (shortly after construction) until June 2015. The pore pressure represents the water pressure near the drain tile elevation near the bottom the GRS fill in both abutments. Results are presented in Figure 49.
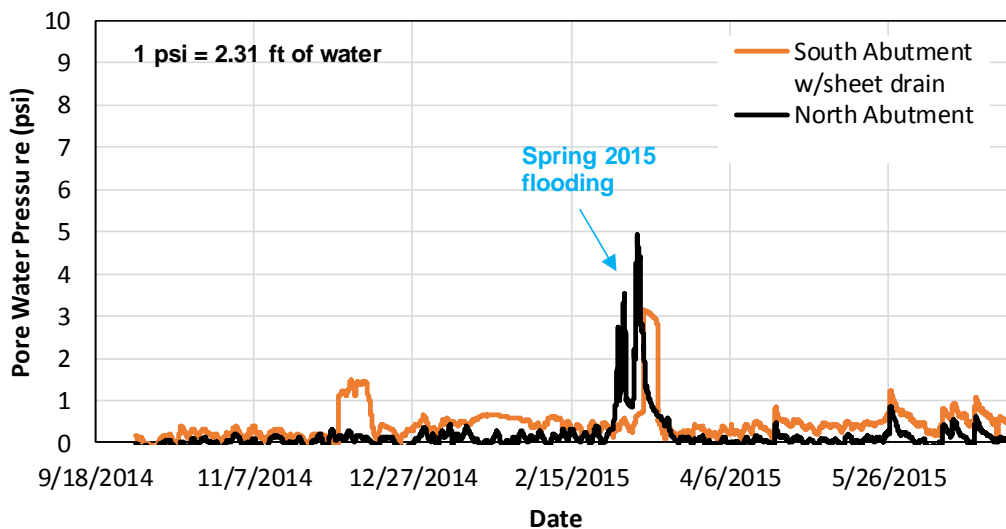
Figure 49. Pore water pressure in north and south abutments

The results captured pore pressure during a spring flood event that occurred in the region with maximum water pressure of about 5 psi and about 11.6 ft of water above the drain tile.

Results showed that from early December 2014, pore pressure generally fluctuated between 0 and 1.0 psi with about 1 to 2.5 ft of water in the south abutment, except during the spring 2015 flooding. On the north abutment, the pore pressure fluctuations were slightly lower, between 0 and 0.8 psi. The reason for this is likely because the sensor location on the south abutment was about 1 ft lower than the one on the north abutment.

During the flood period, a peak pore pressure of about 3.5 psi and about 8.1 ft of water was recorded in the south abutment versus about 5 psi and about 11.6 ft of water in the north abutment.

The most important aspect of the readings is the rate of pore water pressure dissipation between the south and north abutments. For the south abutment, where the vertical sheet drain was installed, the peak pressure during the flood event dissipated from peak to about 0.5 psi within less than 2 days. For the north abutment, the pore pressure dissipation took about 12 days. This suggests that the installation of the vertical sheet drain can help with drainage significantly during a flood event.

4 SUMMARY, CONCLUSIONS, AND RECOMMENDATIONS

4.1 Summary

Recently, there has been increased interest in constructing bridges that last longer, are less expensive, and take less time to construct. The idea is to generally increase the cost-effectiveness of bridges by increasing their durability (i.e., useful life) and minimizing construction disruptions to the traveling public.

A bridge in Buchanan County, Iowa was constructed with innovative concepts to increase its durability while also striving to construct the bridge without the use of vertical lift equipment, making the bridge system an attractive alternative for counties. The innovative concepts utilized in the bridge included HPC made with LWFAs for internal curing, a GRS foundation, and a cast-on-site concrete box-beam superstructure that was intended to be placed using equipment other than a traditional overhead crane.

4.2 Conclusions

- The use of LWFAs for the concrete leads to higher strength of concrete and slightly lower weight of the beams.

- The beam weight was too heavy for the tow truck to slide or lift and led to some minor damage of the test girder.

- Lifting the beams from both ends using two backhoes and moving the beams over the creek was a successful approach and did not cause any damage to the beams beyond some minor bottom flange cracking.

- The load tests performed on the bridge over three years indicated that the bridge joints are well connected and performing well.

- The construction of the beams on-site followed by moving them over the abutments was a time-saving approach, which led to less traffic disruption.

- The GRS abutments did not show any erosion of backfill or any other issues after a flood event occurred in the spring of 2015.

- Results showed that the installation of the vertical sheet drain in one of the abutments provided improved drainage conditions over the abutment without the vertical sheet drain.

4.3   Recommendations

- Using backhoes to lift the cast-on-site beams is recommended.

- Concrete should be cured internally in addition to the external curing.

- Long-term visual monitoring of these two abutments is recommended to see how they perform with additional flood events. A proper scour design was not performed for this site, although the sheet piles were extended at least 5 ft into the very stiff foundation layer. Scouring near the bottom of the sheet piles should be monitored over time.

4.4   Future Study

- The method of cast-on-site beams should be attempted and tested for a longer span or multiple span bridge.

- The lifting of the cast-on-site beams using backhoes may have a limit of span length, which should be investigated.

- A bridge constructed using the philosophy of "get in, get out, stay out" should be inspected for structural soundness for a longer time period.

- The GRS benefits with the inclusion of vertical sheet drains should be further studied for a broader impact using different backfill materials that are typically used in Iowa, with varying fines content and particle size distributions.

REFERENCES

AASHTO. 2012, *AASHTO LRFD Bridge Design Specifications.* American Association of State Highway and Transportation Officials, Washington, DC.

AASHTO. 2014. *AASHTO TP 95: Standard Method of Test for Surface Resistivity Indication of Concrete's Ability to Resist Chloride Ion Penetration.* American Association of State Highway and Transportation Officials, Washington, DC.

ACI. 2016, *Guide to External Curing of Concrete*. ACI 308R-16. American Concrete Institute, Farmington Hills, MI. May 2016.

Adams, M. T., J. E. Nicks, T. Stabile, J. T. H. Wu, W. Schlatter, and J. Hartmann. 2011a. *Geosynthetic Reinforced Soil Integrated Bridge System—Synthesis Report*. Report No. FHWA-HRT-11-027. Federal Highway Administration, Turner-Fairbank Highway Research Center, McLean, VA.

Adams, M. T., J. E. Nicks, T. Stabile, J. T. H. Wu, W. Schlatter, and J. Hartmann. 2011b. *Geosynthetic Reinforced Soil Integrated Bridge System—Interim Implementation Guide*. Report No. FHWA-HRT-11-026. Federal Highway Administration, Turner-Fairbank Highway Research Center, McLean, VA.

ASTM. 2005. *ASTM C39/C39M – 05 Standard Test Method for Compressive Strength of Cylindrical Concrete Specimens*. ASTM International, West Conshohocken, PA.

ASTM. 2011, *ASTM D4595 – 11 Standard Test Method for Tensile Properties of Geotextiles by the Wide-Width Strip Method.* ASTM International, West Conshohocken, PA.

Babcock, A. and P. Taylor. 2015. *Impacts of Internal Curing on Concrete Properties.* National Concrete Pavement Technology Center, Iowa State University, Ames, IA.

Bentz, E. and M. Collins. 2001. *Response-2000*. University of Toronto, Toronto, Canada. Last accessed August 10, 2017. www.ecf.utoronto.ca/~bentz/r2k.htm.

Berg, R., B. R. Christopher, and N. C. Samtani. 2009. *Design and Construction of Mechanically Stabilized Earth Walls and Reinforced Soil Slopes – Volume I*. FHWA-NHI-10-024. National Highway Institute, Federal Highway Administration. Washington, DC.

Mistry, V. and A. Mangus. 2006. Get In, Stay In, Get Out, Stay Out. *Public Roads*. Vol. 70, No. 3.

Taylor, P. C. 2014. *Curing Concrete*. CRC Press, Boca Raton, FL.

Vennapusa, P., D. J. White, W. Klaiber, and S. Wang. 2012. *Geosynthetic Reinforced Soil for Low-Volume Bridge Abutments*. Center for Earthworks Engineering Research and Bridge Engineering Center, Institute for Transportation, Iowa State University, Ames, IA.

APPENDIX. SOIL BORING LOGS AND SLOPE STABILITY ANALYSIS SUMMARY

LOG OF BORING NO. 1

CLIENT	Iowa DOT/Buchanan County	PROJECT NAME		Victor Ave Bridge over Praire Creek
SITE	Victor Ave	PROJECT NUMBER		

Boring located on the south side of the east abutment. - top of existing grade

Depth, ft		DESCRIPTION	USCS SYMBOL	NUMBER	TYPE	RECOVERY, in.	SPT-N BLOWS / ft.	WATER CONTENT, %	DRY UNIT WEIGHT, pcf	UNCONFINED STRENGHT, psf	OTHER
4	7	Dark Brown Silty Sand	SM	1	SS		5				PL=26, LL=33, PI =7
8		Grey Sandy Lean Clay	CL	2	SS		5				PL=15, LL=27, PI =12
12	12										
	14.3			3	ST	22.25		19.4, 17.9	113.1	2464.5*	
16	17			4	SS		14				
20	22.3	Light Grey to Grey Sandy Lean Clay	CL	5	ST	24.75		15.2	118.5	31579	PL=17, LL=30, PI =13
24	24			6	SS		14				
	27			7	SS		15				
28				8	SS		20				
32	32										
36	37		CL	9	SS		22				PL=16, LL=30, PI =14
40	42	Grey Sandy Lean Clay		10	SS		20				
44	47			11	SS		26				
48				12	SS		22				
52	52										
		BOTTOM OF BORING									

The stratification lines represent the approximate boundary lines between soil and rock types; in-situ, the transition may be gradual.

LL = Liquid Limit, PI = Plasticity Index, * Average of two measurements (2049 psf and 2850 psf)

WATERLEVEL OBSERVATIONS, ft	BORING STARTED		LOGGED BY	
WL ⊽	BORING COMPLETED		RIG	
	DRILLED BY		APPROVED BY	

CENTER FOR CEER EARTHWORKS ENGINEERING RESEARCH

Figure 50. Log of Soil Boring 1 on south side of east abutment

LOG OF BORING NO. 2

CLIENT	Iowa DOT/Buchanan County	PROJECT NAME	Victor Ave Bridge over Praire Creek
SITE	Victor Ave	PROJECT NUMBER	

Boring located on the south side of the west abutment. - top of existing grade

Depth, ft	DESCRIPTION	USCS SYMBOL	NUMBER	TYPE	RECOVERY, in.	SPT-N BLOWS / ft.	WATER CONTENT, %	DRY UNIT WEIGHT, pcf	UNCONFINED STRENGHT, psf	OTHER
4	Dark Brown Clayey Sand	SC	1	SS		15				PL=21, LL=29, PI =8
7										
8			2	SS		8				
12 (12)	Light Grey to Grey Sandy Lean Clay									
16		CL	3	SS		12				PL=16, LL=30, PI =14
17.0										
20			4	SS		14				
22.0										
24			5	SS		16				
24.1										
28			6	SS		18				
29.1										
32			7	SS		22				
34.1	Grey Sandy Lean Clay									
36			8	SS		20				
39.1										
40			9	SS		20				
44 (44.1)										
48			10	SS		19				
51.1										
52	BOTTOM OF BORING									

The stratification lines represent the approximate boundary lines between soil and rock types; in-situ, the transition may be gradual.

c' = Effective Cohesion and *φ'* = Effective Friction Angle, LL = Liquid Limit, PI = Plasticity Index

	WATERLEVEL OBSERVATIONS, ft	BORING STARTED		LOGGED BY	
CENTER FOR **CEER** EARTHWORKS ENGINEERING RESEARCH	WL ▽	BORING COMPLETED		RIG	
		DRILLED BY		APPROVED BY	

Figure 51. Log of Soil Boring 2 on south side of west abutment
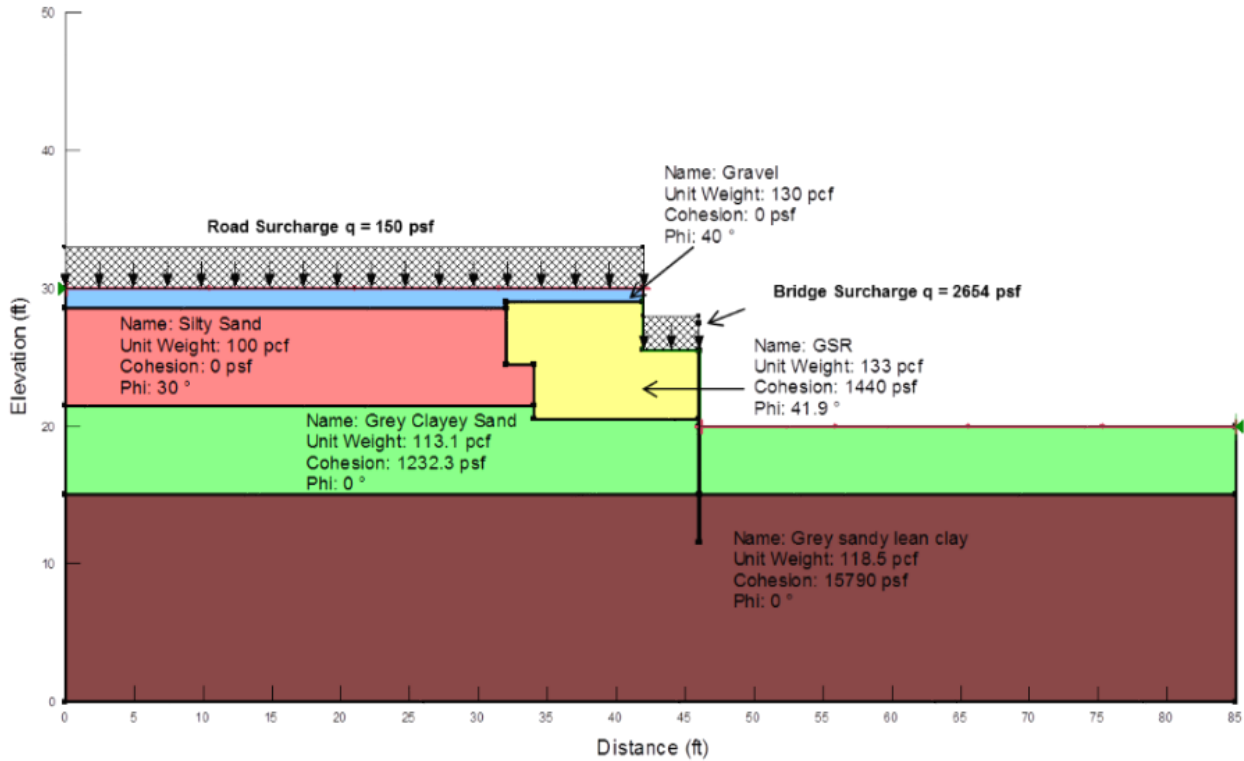
Figure 52. Soil cross-section profile setup for slope stability analysis

Table 8. Slope stability analysis summary

Description	Method Morgenstern-Price	Janbu	Bishop
No Sheet Pile Cases			
Low water table (near stream bed)	1.563	1.513	1.549
High water table (near bottom of bridge deck)	0.481	2.049	1.874
Rapid draw down	0.484	1.784	1.602
Cases with Different Sheet Pile Lengths			
Low water table w/sheet pile ~5 ft into gray clayey sand	1.463	1.449	1.457
Low water table w/sheet pile ~10 ft into gray clayey sand	7.833	6.907	8.375
Low water table w/sheet pile into gray sandy lean clay	13.288	11.755	13.669
High water table w/sheet pile ~5 ft into gray clayey sand	1.602	1.566	1.589
High water table w/sheet pile ~10 ft into gray clayey sand	8.881	7.821	9.411
High water table w/sheet pile into gray sandy lean clay	15.217	13.673	16.046
Rapid drawdown w/sheet pile ~10 ft into gray clayey sand	1.400	1.367	1.388
Rapid drawdown w/sheet pile ~5 ft into gray clayey sand	7.824	6.871	8.210
Rapid drawdown w/sheet pile into gray sandy lean clay	13.827	12.274	14.228

Highlighted=actual used in design/construction